COOKOFF PROTOCOL FOR MUNITION ASSESSMENT

Andrew C. Victor
Victor Technology
1537 Fourth St., Suite 218
San Rafael, CA 94901

PRELUDE

The methods presented in this protocol were developed over several years and successfully applied to design and analysis of a number of munitions and a number of energetic material (EM) laboratory-scale tests. Before the protocol can be applied with high confidence to new energetic material, it must be tested for high-temperature behaviors and properties that are obvious throughout the sections of the protocol.

The original approach to developing these methods was based upon protocol flowcharts developed by The Technical Cooperation Program W Action Group-11 (TTCP WAG-11) and then taken over for upgrading, maintenance, and distribution by the NATO Insensitive Munitions Information Center (NIMIC).

INTRODUCTION

Cookoff is usually thought of in terms of the specific tests that a munition must pass to meet specified safety standards and the manner in which these tests are conducted. These tests are the slow cookoff test (in which the munition is heated at a rate of 3.3°C/hr) and the fast cookoff test with heating in a hydrocarbon liquid-fuel fire or wood-fueled bonfire. The intent of these tests is to ensure that a munition will have a certain level of safety in a real thermal hazard environment. In compliance with requirements that Threat Hazard Assessment be performed as part of the safety (insensitive munitions) protocol, these tests are increasingly being performed with the munition confined inside shipping containers or launchers, as appropriate to the logistic or operational environments in which slow or fast heating threats are considered most likely to occur. Thus the bare munitions may actually be exposed to a wide range of heating rates in the standard tests, as actually performed. A much wider range of heating rates is expected in the actual threat environment. The purpose of this protocol is to outline methods for assessing the response of munition systems to any cookoff environment, including the required tests and real accidents. This protocol aims to predict the response of a munition to a given thermal stimulus, both in terms of initiation of combustion reactions and output or violence of the reactions. (When and where does a reaction occur in the energetic material and how violent is the reaction?) The protocol is shown in flowchart form in Figure I-1. Phenomena listed under Inert Material Behavior (Section 3) in the flowchart have critical couplings (too complex to show in a single page chart) to items listed under Energetic Materials (Sections 4, 5, 6, 7, and 8). Technical descriptions and analytical calculation methods follow in the remainder of this protocol with explanation of these couplings and some test cases for demonstration.

The flowchart can be used as the basis for developing a general-purpose numerical cookoff code. However, there are so many possible scenario-dependent choices of relationships between inert and energetic material behavior at an intimate level that preliminary analyses using analytical relationships are recommended where possible. Numerical methods must be used for time-dependent heat transfer calculations in order to obtain values of T(x, t) in inert and energetic components. For unsymmetrical heat sources, two- or three- dimensional numerical codes will ultimately be required. However, for coupled numerical-analytical solutions, one-dimensional (1-D) numerical codes that approximate the munition geometry (cylindrical or spherical) provide adequate values of T(r, t) for many very good engineering-level solutions.

1. SCENARIO

Complete description of the scenario is the first step in a thermal analysis of munition heating and reaction. The term "munition system" is used to include the munition and all external components that accompany it in the scenario. These components may include a shipping container, launcher, lugs, fins, and if appropriate, thermal shields or barriers between the munition system and the heat source. In the absence of dynamic mechanical behavior of these inert surrounds, they can be analyzed in separate heat transfer calculations to obtain a heating rate for the munition itself or even for the surface of the energetic material (EM) charge.

Report Documentation Page

Form Approved
OMB No. 0704-0188

1. REPORT DATE	2. REPORT TYPE	3. DATES COVERED
AUG 1996		**00-00-1996 to 00-00-1996**

4. TITLE AND SUBTITLE	5a. CONTRACT NUMBER
Cookoff Protocol for Munition Assessment	5b. GRANT NUMBER
	5c. PROGRAM ELEMENT NUMBER
6. AUTHOR(S)	5d. PROJECT NUMBER
	5e. TASK NUMBER
	5f. WORK UNIT NUMBER
7. PERFORMING ORGANIZATION NAME(S) AND ADDRESS(ES) **Victor Technology,1537 Fourth St., Suite 218,San Rafael,CA,94901**	8. PERFORMING ORGANIZATION REPORT NUMBER
9. SPONSORING/MONITORING AGENCY NAME(S) AND ADDRESS(ES)	10. SPONSOR/MONITOR'S ACRONYM(S)
	11. SPONSOR/MONITOR'S REPORT NUMBER(S)

12. DISTRIBUTION/AVAILABILITY STATEMENT
Approved for public release; distribution unlimited

13. SUPPLEMENTARY NOTES
See also ADM000767. Proceedings of the Twenty-Seventh DoD Explosives Safety Seminar Held in Las Vegas, NV on 22-26 August 1996.

14. ABSTRACT

15. SUBJECT TERMS

16. SECURITY CLASSIFICATION OF:			17. LIMITATION OF ABSTRACT	18. NUMBER OF PAGES	19a. NAME OF RESPONSIBLE PERSON
a. REPORT	b. ABSTRACT	c. THIS PAGE			
unclassified	**unclassified**	**unclassified**	**Same as Report (SAR)**	**31**	

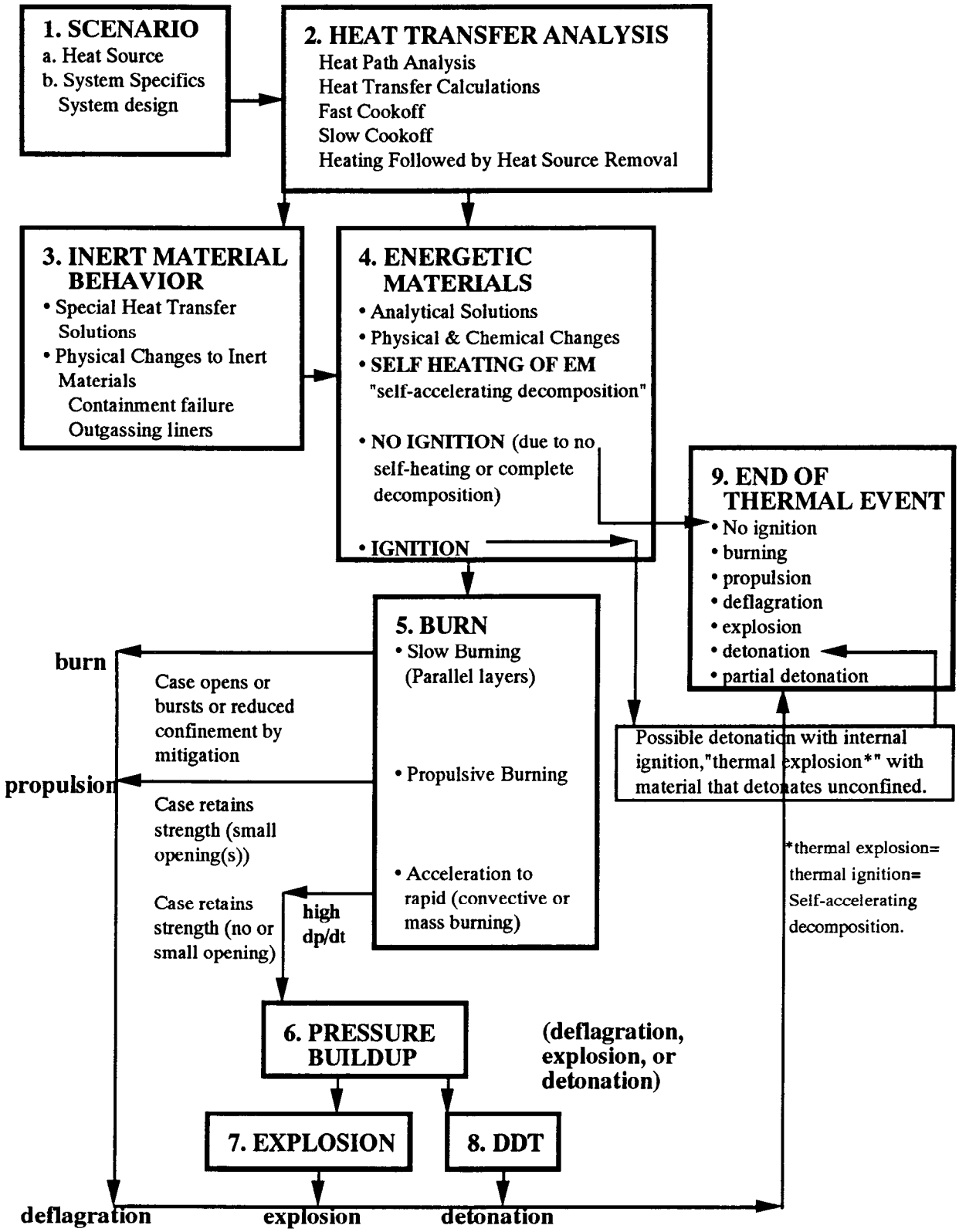

Figure I-1. Cookoff protocol schematic diagram

a. HEAT SOURCE

The heat source and the munition system's relation to it must be completely described spatially. The temperature of the heated medium on the outer boundary of the munition system is given as a function of time. For three-dimensional analysis, the time dependence of the temperature will be given for all applicable coordinates. For example, for a cylindrical munition, T (r, z, ϕ t) is appropriate. For a simpler two dimensional analysis, the analyst will have to make a choice of two of the three spatial coordinates that depends on the characteristics of the heat source and the munition design. For a one-dimensional analysis, which is often adequate for straightforward cylindrical munition geometry, T (r, t) will generally be used, although in some cases or in some parts of the analysis T (z, t) or T (ϕ, t) may be preferable (see section 3). However, caution is critical in selecting a reduced axis set. For example, it is clear that selecting radius, r, as the only spatial variable when analyzing a cylindrical munition will ignore end effects (which may not be important for problems in which time to cookoff and temperature history of inert external parts are important). When performing a two-dimensional analysis using the axes r and z, the analyst must be certain that the problem is set up in cylindrical coordinates – not cartesian coordinates; if the cartesian coordinate x is accidentally substituted for the radius, r, serious calculational errors will occur for slow-heating scenarios. On the other hand, for fast-heating scenarios, in which only a thin shell at the outer surface of the EM is heated, substitution of x for r makes virtually no difference in the end result.

For a munition system submerged in a flame, heating by radiation is a major heat transfer mechanism. For such a flame, the heating rate of the surface of the munition system can be approximated by equation (1-1). The first term in equation (1-1) is the radiation heating term with the quantum constants included; the second term is the convection heating term with the convective heat transfer coefficient h = 0.006 KW/m^2-°C.

$$Q = 60\,(\varepsilon_f\,\varepsilon_s(T_f/1000)^4 - \varepsilon_s(T_s/1000)^4) + .006\,(T_f - T_s),\ KW/m^2 \qquad (1\text{-}1)$$

where: T_s = munition surface temperature in Kelvins (K).

T_f = flame temperature, K.

ε_f, ε_s = flame and surface emissivities, respectively.

For opaque flames of hydrocarbon fuel fires or wood bonfires, which have emissivity values approaching unity, radiation predominates and heating of the outer surface by convection or conduction can be virtually ignored. For such flames, the surface of the munition system is often covered with soot during the early phases of heating and a unity value of surface emissivity can be used too. For a munition fully engulfed in a sooty fire, a one-dimensional heat-flow calculation is sufficient. However, many test fires do not fully engulf the munition because of ambient wind effects and non uniform circumferential heating occurs. As a rule, if the munition can be seen through the flames during a test, it will be subject to both temporal and spatial heating fluctuations.

For transparent flames of propane or natural gas fires, lower values of both flame and surface emissivities will cause lower heating rates of the munition system and increase the importance of the convection term. Because of this, there is a greater lack of symmetry in the surface heat transfer rates with gas flames than for liquid-fuel flames.

There is also lack of symmetry in heating patterns in thermal threat scenarios involving heat impingement from a huffer, rocket motor exhaust plume, or torching from a burning rocket motor or warhead as well as for munitions only partially submerged in a flame.

For slow cookoff scenarios, exemplified by the 3.3°C/hr heating rate of the slow cookoff test, little error is introduced if the munition surface is assumed to heat at the same rate as the ambient air. In this case, heat transfer is calculated simply with a time-dependent conductive heat transfer calculation using the rising temperature of the heated oven air as a "driving force." For direct exposure of bare munitions to slow heating, it is often possible to ignore the thermal resistance of a metal case and apply the temperature rise rate of the ambient air directly to the outer surface of the charge with little loss in accuracy.

As one examines heating rates greater than 3.3°C/hr, the thermal resistance of inert layers enclosing the charge become increasingly important and must be included in the heat transfer analysis. For example, in slow cookoff tests using steel motor cases, the case temperature at the time ignition occurred was only about 1°C cooler than the air at a heating rate of 3.3°C/hr, but about 30°C cooler at a heating rate of 42°C/hr.[1] For such scenarios, values of convection and conduction heating of the surface of the munition system must be calculated as a function of time. At small temperature differences, radiation heating can be ignored, however it can tested for to verify that assumption. The specific source of the indirect slow (or intermediate rate)

heating should be identified to determine a credible description of the heat source in space and time – is it a nearby fire, a fire in an adjacent compartment, etc. – to determine appropriate heat-transfer mechanisms.

The initial temperature distribution (thermal profile) within the munition system is usually chosen to be uniform and the same as the starting temperature of the test. However, this assumption should be modified if the test or scenario to be simulated in the calculation is preceded by a preheating phase or if the munition has experienced some period of prior heating or cooling by the environment.

b. SYSTEM SPECIFICS

A detailed engineering drawing of the munition system should be studied to obtain information on geometric and size relationships and materials. One or more munitions may be considered to comprise the munition system, however, it is recommended that the system analyzed include no more than one container or launcher load of munitions. Appropriate thermal and mechanical properties of the inert and energetic materials must be obtained. For example, if one is doing a slow cookoff (3.3°C/hr) analysis of a munition system with aluminum parts, weakening and melting of those parts are not likely to occur. However, at higher heating rates, those parts will experience higher temperatures and these effects may occur. In fires, outer aluminum parts often melt prior to ignition of the EM, and this effect must be included in the analysis.

The material properties that must be included in the analysis are listed in Table 1-1. Values of these properties should be known as functions of temperature and to a lesser degree, for some of them, functions of pressure. Without going into greater detail at this stage, some of these properties may experience extreme changes during heating that will affect the outcome of a thermal scenario. Other properties will vary only slowly with temperature, and in many cases those variations can be ignored. Knowledge of the reaction level obtained with the unconfined energetic material (EM) is important. Some EMs detonate unconfined as their response to cookoff testing and are thus extremely hazardous to use without some fail-safe active mitigation device or concept that assures they will be ignited by some other source than their own self-heating. This source may be a specifically-designed mitigation system or just another energetic material within the munition, usually external to the more sensitive one. Some other EMs expand to form a foamy substance with decomposition-product gas trapped in internal voids. AP/HTPB propellants are a notable example of this. When these foamed propellants are ignited in even moderately strong enclosures (z.b., rocket motor cases), either by a designed igniter or due to their own self-heating, very violent reactions occur (see Sections 5 and 6).

Other factors include whether the munition system is in a confined space that will restrict convective flow and reduce debris throw in a violent reaction. If the munition system is unconfined, airflow across it will affect burning of a fire or uniformity of indirect heating. Igniters or booster explosives, if more thermally sensitive than the main charge, can determine the reaction that will ensue.

2. HEAT TRANSFER ANALYSIS

Using the material property values, a preliminary assessment of anticipated scenario events should be done. A cursory heat-path analysis should be part of this assessment. For complex munition systems, for example, those comprised of multiple munitions in a single container or launcher, one of the first steps in the preliminary assessment should be to determine if the analysis can be reduced to consideration of a simpler geometry and a single munition without losing information critical to the outcome.

For example, consider fast cookoff of an unshielded ("bare") munition treated with the preferential insulation technique (PIT) – an intumescent coating on the entire munition except for one or more strips of exposed bare case metal about 5 cm wide. A preliminary assessment should obtain approximate heat transfer rates into the energetic material for the two types of covering. Strength estimates of the hotter metal region would be obtained; some circumferential heat transfer estimates in the metal case would be made; stress concentrations would be calculated; if there is an out-gassing liner, its contribution to the stress would be included.

Another example might be a rocket motor with a metal case, separated from the propellant by a thin liner or insulation, and with metal bulkheads attached to the case and supporting a complex internal charge and nozzle structure. The primary question for the heat-path analysis is to determine if the metal bulkheads will bring heat to internal propellant surfaces faster than the transfer through the liner to the outer propellant surface.

Table 1-1. Material Properties Needed for Cookoff Analysis

Properties (T)	Inert Materials	Energetic Materials
geometry	X	X
dimensions	X	X
bulk density	X	X
heat capacity	X	X
thermal conductivity	X	X
melting point	X	X
heat of fusion	X	X
sublimation point	X	X
heat of sublimation	X	X
mechanical props (low and high rate) (modulus, yield strength, σ/ε, fracture (T))	X	X
activation energy		X
preexponential factor		X
heat of decomposition		X
cookoff reaction level of unconfined EM (burn, explode or detonate)?)		X
void configuration of EM (foam, etc.)		X
"break-point" pressure or dP/dt for convective (mass) burning		X
composition of interstitial gas	X	X

Other considerations are the possibilities that a heat path through the nozzle of a rocket motor may cause ignition or that ignition may start in EM that has exuded from the munition case. Either of these will change the heat transfer analysis significantly. Similar, is consideration of combustible components of the munition system – other than the EM. For example, fibers or resins of some composite case, launcher, or container materials.

Finally, consider a cylindrical launcher, canister, or container with multiple layers of munitions in a close-packed arrangement. Heat-path analysis is important to determine how well a single munition in a cylindrical enclosure (a one-dimensional analog) can be used to model the time-to ignition and critical component temperatures in a simple way. The heat-path analysis will give order-of-magnitude estimates of how the heat flows from the outer to inner components and how much (if any) reduction of heat concentration must be accounted for in the one-dimensional analog.

These heat-path analyses might use "back of the envelope" calculations, if possible, in which the time-dependent effects are only approximated. The result of each analysis will be an outline of the detailed heat transfer analysis steps necessary to include the important effects. The alternative is to use a full-blown three-dimensional numerical code that accounts for every possible effect over all regions of an entire munition system. To use such a code routinely would require that it contain all possibilities for all possible munition systems – a costly, inflexible option.

Many munition systems will be simpler than the examples just given. For these it may be intuitively obvious that a one-dimensional cylindrical or spherical heat-transfer analysis will be adequate to predict time-to-ignition and the time-dependent thermal profile. However, even for these systems the initial heat-path analysis should be used to determine if extreme material behaviors may be encountered that will affect the analysis (and in fact should result in design changes); for example: (1) Will some inert parts degrade in strength or melt? (2) Will liner outgassing be important? (3) Will EM foaming occur and change the thermal properties of the charge used in latter times of the calculation? (4) Are there undesired heat paths that may cause an excessively violent reaction?

HEAT TRANSFER CALCULATIONS

The primary goals of the heat transfer calculations in a cookoff analysis are to determine the time-to-ignition or "time-to-cookoff," physical changes in munition-system components during heating, and the thermal profile of the munition system as a function of time. A physical description of the munition is important. For example, the physical state of the inert and energetic materials: (1) Has the case been burst by internal

pressure? (2) Has an active or passive mitigation device functioned, and with what effect? (3) Has case material melted? (4) What are the strengths or stress-strain relationships of critical confining case components? (5) Has energetic material melted? May it have flowed from the case? A time-stepped (or phased) analysis may enable one to answer these questions for times prior to ignition; this can be very important since these events may cause ignition to occur outside the munition case. Elementary heat-flow analysis techniques, as given in the limited list of references,[2-6] can be very useful. A numerical (finite-difference or finite element) heat-transfer code[7] may be used as part of the analysis or it may be specially adapted to perform both heat-flow calculations and executive control functions for the other events.

For configurations that can be realistically equated to one-dimensional planar, cylindrical, or spherical geometries, personal-computer spreadsheet models have been successfully used as the framework for one-dimensional numerical models that predict time-to-ignition for heating rates as low as 3.3°C/hr and as high as those encountered in direct flame impingement on the bare munition. The main consideration in choosing a shape in the one-dimensional analog is to closely approximate the surface area to volume ratio of the component being analyzed and thus a similar ratio between heat input and internal heat flow (not possible for angular geometries such as rectangular boxes where heat concentrations at the corners may be critical). Therefore, reasonable values of heat transfer through container, launcher, and even munition case walls can be obtained using planar models as well as cylindrical or spherical models. Within the munition itself, in slow cookoff scenarios, as heat concentrates toward the center of the charge, a closer simulation (i.e., cylinder or sphere) is necessary.[8]

Using one-dimensional models, the heat transfer through reasonably conductive walls (aluminum, steel, and graphite/epoxy composite) can usually be treated in a single step. This approach also seems to work for thin liner or insulation layers. Wall materials with higher resistance "stiffen" the equations and can create calculational problems. Physically, these materials resist heat flow quite effectively and some time may pass between initial heating of their outer surface and the inward flow of heat from their inner surface. This can be overcome by dividing the layer into a number of calculational shells (at a high cost in RAM needed to calculate heat transfer in the energetic material – if the entire munition system is calculated in a single run). Alternatively, the temperature distribution within the resistive wall can be described by an error function (available in the function libraries of many spreadsheets and described in Section 3) that is used to establish the initial temperature gradient and heat transfer rate to its inner surface.[3,6] Once the inner surface temperature starts to rise, a linear function can be used subsequently to calculate heat transfer through the wall. Because of the shape of the error function, the wall should probably be described subsequently by a grid with a minimum of two or three shells to maintain calculational stability, although this may not be necessary and can be tested for in preliminary calculations.

For very resistive walls exposed to very high temperatures (for example, intumescent coatings on the outside of munition systems exposed directly to flames), the temperature rise of the inner wall can be taken directly from measured backface-temperature data and used as the temperature rise rate of the outer surface of the next layer (i.e., the metal wall of the munition or launcher). This can be done either graphically or using simple algebraic equations (see Section 3).

In fast cookoff scenarios, some inert materials of the munition system may degrade at the exposure temperatures. For example, aluminum melts at 933 K and composite materials will char and their plastic matrix burn at lower temperatures – for some, the entire composite structure will degrade. This can be accounted for easily by subroutine programming in a FORTRAN code. In a spreadsheet code, there are two ways to account for the degradation of materials; either include an IF statement in the cell and the equations both with and without degradation of the material, or rerun the spreadsheet and modify the equations in the appropriate column after the failure point of the material has been reached. For completeness, some kinetic aspect of the degradation should be included (such as the heat of fusion of aluminum) so the calculated process will occur on a realistic time scale that accounts for thermal capacity. Following total loss of a structural component to the flame, the flame is then calculated to transfer heat directly to the next layer. This process can be repeated until all degradable structures are removed or the EM ignites.

During the time that inert components are heating, the inner EM is being heated too. The entire heating process occurs "in phase," so to speak, and although all the numerical techniques calculate the heating process in phase, it is not necessary to calculate it that way. Simple heat transfer calculations can be applied to the outer inert materials, making sure that all heat balances are maintained, and the heating rate of the outer EM surface (or inner inert surface) can be calculated. If the heating rate of the EM surface is determined, a single analytical expression (equation (4-1)) can be used to predict the ignition temperature and time to cookoff.

The numerical techniques predict runaway temperature rise of the EM at the appropriate time because the exponential self-heating term is included in the heat-transfer equations. In the one-dimensional spreadsheet models, ten radial grid points (i.e., ten shells) within the EM have always given good results, and in many cases only five shells have been necessary. For fast cookoff scenarios, these shells should be concentrated near the EM outer surface. As a rough rule of thumb, the total thickness of the calculational layer need be no greater than $x = \sqrt{(\alpha\ t')}$ where t' is time in seconds, and α is the thermal diffusivity of the EM, described later. For a grid of fixed dimensions, t' should be the time to cookoff.

Once ignition of the energetic material occurs, the scenario enters a more dynamic phase that requires completely different types of calculations to predict whether a relatively mild burning reaction results or more violent "deflagration," explosion, or detonation reactions follow. At the present time, verified calculation methods for predicting such reaction levels do not really exist.

During the dynamic phase, heat transfer calculations are no longer of concern except (conceptually) for the complex scenario in which one is interested in studying the interactions of a group of munitions. Currently, it is recommended that such complex scenarios be modeled by assuming the reaction of one of the munitions as the starting point rather than linking codes in what might be considered to be multiple scenarios.

FAST COOKOFF

Equation (1-1) is used as the initial heating rate of the surface exposed to flame in fast-cookoff scenarios. This heat flux is initially many times greater than would be obtained by assuming an initial heat flux from an outer wall at the nominal flame temperature (typically 1,144 K) flowing by conduction to an inner wall at ambient temperature (for example, 294 K), and that is why using a realistic value for the heat flux is so critical. In open propane burner tests, the measured heat flux values are about one-half the magnitude of those in liquid hydrocarbon fuel fires, are more strongly dependent on direction, ϕ, and are consistent with reduced flame emissivity and a more significant convection heat transfer mechanism. It has been estimated that propane or methane flames of about 1,533 K would be necessary to provide heat flux equivalent to that from smoky flames at 1,144 K.[9]

Because the thermal conductivity of the metal case is at least 100 times higher than that of the liner or energetic material immediately in contact with its inner surface, as a first approximation, the case wall temperature rise can be approximated by ignoring heat flux from its backwall (Q_{liner}, which ranged from < 2% to 7% of the influx). However, the backwall heat loss must be considered with low conductivity cases. Ignoring the backwall heat flux in equation (2-1) reduces calculated time-to-cookoff (i.e., time to ignition) by only about 3% for metal cases.

$$T_{ave} = T_{ave(t-\Delta t)} + (Q' - Q_{liner})\,\Delta t / (C_{pcase}\,\pi\rho(R_o^2 - R_i^2) \qquad (2\text{-}1)$$

where: T_{ave} = average case wall temperature. The subscript, $(t-\Delta t)$, represents condition at previous time step. $T_s = T_{ave} + \Delta T/2$, see equations (1) and (3).
R_O = outer case wall radius.
R_i = inner case wall radius.
$Q' = 2\pi\ R_O\ Q$ (assuming unit length cylinder)
C_{pcase} = specific heat of case material
Δt = time step used in step-by-step calculation.

The temperature gradient through the case wall is given by the usual cylindrical heat flow equations (2-2) and (2-3), although for the thin layers one is usually concerned with in fast cookoff, planar heat conduction equations give about the same result.

$$\Delta T = Q' \ln (R_O / R_i) / 2\pi\ \lambda_{case} \qquad (2\text{-}2)$$

where: λ_{case} = thermal conductivity of case.

The heat flux through the liner/insulator is calculated by:

$$Q_{liner} = 2\pi\ \lambda_{ins}\ \Delta t\ (T_{ave} - \Delta T/2 - T_{liner(t-\Delta t)}) / \ln (R_i / R_p) \qquad (2\text{-}3)$$

where: λ_{ins} = thermal conductivity of liner.
$T_{liner(t-\Delta t)}$ = temperature of inner surface of liner or outer propellant/explosive surface.
R_p = radius of inner liner surface or outer propellant/explosive surface.

Finally, the propellant/explosive surface and near-surface temperature is approximated by considering Arrhenius kinetics by using equations (2-4) and (2-5) for several grid shells into the energetic material. These are the equations of steady-state heat transfer for infinite cylinders, framed in time-steps that "boot-strap" to useful solutions if the energy transfer into all cells remains positive.[8]

$$Q_n = \pi(t_k - t_{(k-1)}) \{(2\lambda (T_{n_k} - T_{(n+1)(k-1)}) / \ln (R_n/R_{(n+1)}) + \rho Q Z (R_n^2 - R_{(n+1)}^2) \exp(-E/(R(T_{n_k} + T_{(n+1)(k-1)})/2)) \} \quad (2\text{-}4)$$

$$T_{(n+1)} = T_n + Q_n / (\pi \rho C_p (R_n^2 - R_{(n+1)}^2)) \quad (2\text{-}5)$$

The outer wall temperature of the energetic cylinder, To_k, is set for each time step by equation (2-2) or by raising the temperature at the desired heating rate. The time step size can be changed during the calculation.

The heat flow through each shell of energetic material is calculated. In the same model, shell self-heating due to energetic material decomposition is calculated if the temperature has risen to the point where that term is significant. This resets the temperature at the inner wall of the shell. The calculation moves inward to the next shell. The outer boundary temperature is assumed to be independent of any internal heating occurring in that time step. However, each shell is subject to radial heat flow from either direction. At some point in the calculation, self-heating takes over and accelerates rapidly in one or more grid zones. When this is interpreted as representing ignition of the propellant or explosive (usually by a sudden "vertical" temperature rise rate), the calculation agrees extremely well with measured data (time to ignition and outer case wall temperature at ignition). Because of the low thermal conductivity values of energetic materials, very steep thermal gradients will initially be generated near the outer energetic material surface. To allow for this, either an error function formulation (see section 3) or calculational shell thicknesses of order $\alpha t/2$ to $\alpha t/3$ must be used near the outer surface (where t is the time in seconds to ignition). Use of larger radial steps, such as dividing the cylinder radius into 5 or ten steps of equal Δr, which works perfectly well for slow cookoff calculations, will result in high estimates of ignition temperature and time-to-ignition for fast cookoff calculations.

The steady-state cylindrical equations are discontinuous at the origin (radius, R = 0). This is no problem for items with a center perforation or bore, such as most rocket motors. However, for most explosive warheads, and other solid test items, this difficulty is overcome by using as small a bore as possible in calculations for solid objects.

Equations (2-1) through (2-5) represent a one-dimensional numerical solution of the Frank-Kaminetskii differential equation (2-6). When the reaction heating term (the right side of equation (2-6)) is zero, the equation is just the well-known heat flow equation.

$$-\lambda \nabla^2 T + \rho C_p (dT/dt) = \rho Q Z w e^{(-E/RT)} \quad (2\text{-}6)$$

(The Laplacian operator ∇^2, in the special cases of spheres, infinitely long cylinders, and infinite slabs, reduces to $\nabla^2 T = (\partial^2 T/\partial x^2) + (m\, \partial T/x \partial x)$.)

where: λ = thermal conductivity, cal/s-cm-K

T = temperature, K — E = activation energy, cal/mole

ρ = density, g/cm^3 — R = gas constant, 1.987 cal/mole-K

C_p = specific heat, cal/g-K — Q = heat of reaction, cal/g

Z = collision number, sec^{-1} — α = thermal diffusivity = $\lambda / \rho C_p$

w = mass fraction of undecomposed energetic material, = 1 for 0th order solution.

m = shape factor: 0 for slabs, 1 for cylinders, and 2 for spheres.

Equations (2-2) through (2-5) can be replicated for use with multiple-layer symmetrical munition systems such as a warhead within the missile skin mounted within a launch tube within a launcher. For the example calculation shown in Figure 2-1, the launcher was assumed to be submerged in a flame that approximated the measured flame temperature as shown ("fire"). This calculation accounted for melting of the aluminum launcher skin and aluminum launch tube (but not the aluminum missile skin). When those components reached a temperature of 933 K, the heating calculation was continued until one-half the latent heat of fusion for the mass of aluminum was absorbed. At that time, the aluminum was assumed to degrade sufficiently for direct contact of the flame with the next inner surface to occur. The calculations as shown (287 seconds) match almost exactly the 290 seconds to ignition measured in a fuel-fire test of the identical

missile system. In addition, thermocouple data confirmed the temperature-time curve calculated for the first half of launch tube heating, following which irregularities in the thermocouple data indicate that the thermocouple probably became detached from the tube surface. For thin internal air gaps, thermal conductivity of the air at appropriate temperatures will be of the order of λ = 0.06 to 0.07 W/m-°C (or as shown in Table 2-1). Table 2-1 gives consistent values of thermal-property constants for a number of inert and energetic materials for use in the thermal calculations of this protocol. More information on energetic material behavior during rapid heating is given in Section 4.

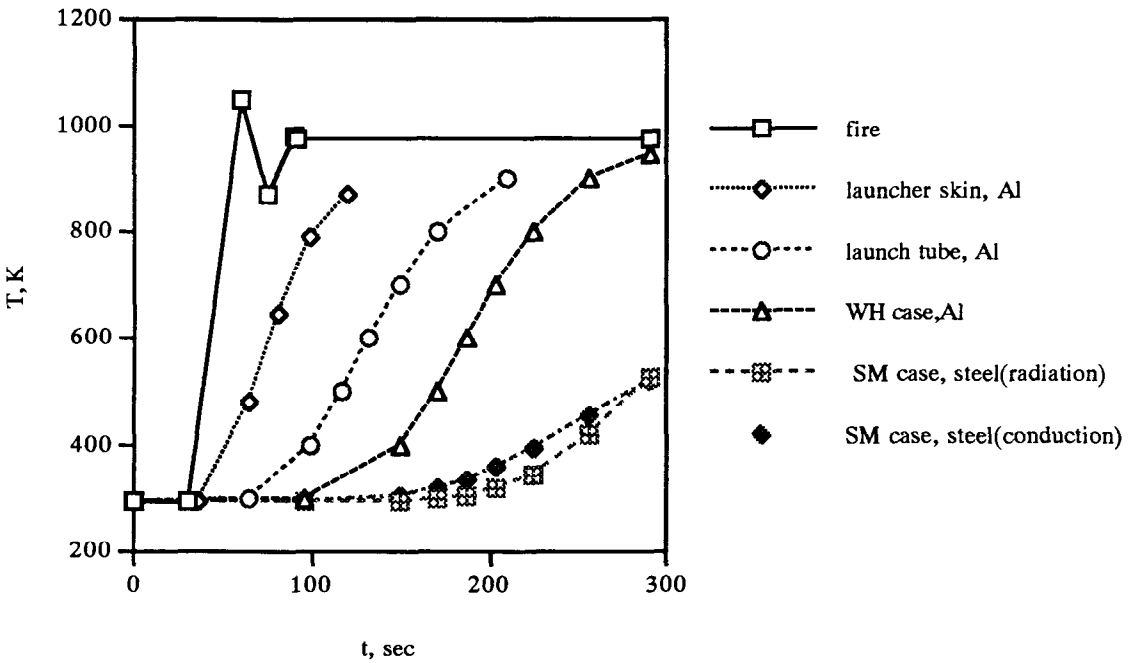

Figure 2-1. Fast cookoff calculations for PBXN-107-containing submunitions (SM) of 2.75-inch diameter warhead (WH) in launch tube within launcher. Curves labeled "SM" represent two methods of calculating heat transfer from warhead case to submunitions; final temperature is calculated interior SM case wall temperature at which the explosive ignited.

SLOW COOKOFF

Slow cookoff and intermediate-rate cookoff calculations also involve numerical solution of equation (2-6). The only differences from fast cookoff are that the boundary conditions will generally be based on either convective or conductive heating of the outer boundary of the munition system. For convective heating of a boundary in still air, a film coefficient h = 0.0094 KW/m^2-°C (0.0134 cal/cm^2-K) is suggested. For convective heating of a boundary in air moving with a velocity of 7 m/s, h = 0.034 KW/m^2-°C (0.048 cal/cm^2-K) is suggested. For thin internal air gaps, thermal conductivity of the air at appropriate temperatures will be of the order of λ = 0.04 to 0.05 W/m-°C (or as shown in Table 2-1). For a bare munition with a metal case and little insulation heated at a rate of 3.3°C/hr, little error is made if the temperature of the outer boundary of the charge is assumed to rise at the same temperature as the environment (i.e., 3.3°C/hr).

When a munition is heated slowly, the outer surface temperature rises faster than at any other location in the munition until at some time self-heating and low thermal diffusivity cause inner temperatures to exceed outer temperatures and runaway self-heating proceeds to ignition. Calculated results showing this behavior are shown in Figure 2-2 for bare cylindrical charges of RDX explosive. The corresponding calculated internal thermal profiles are shown in Figure 2-3. More information on energetic material behavior during slow heating is given in Section 4.

Table 2-1. Thermal Phenomena: Critical Temperatures* and Parameter Values.

Explosive	T_{cr} (°C)	ρ (g/cm^3)	Q (cal/g)	Z (s^{-1})	E(kcal/m)	$\lambda x10^4$(cal/cm/s/K)	C (cal/g/K)	T_d°C**
HMX	253	1.81	500	5 (19) #	52.7	7.0	.27	287
RDX	215	1.72	500	2.015 (18)	47.1	2.5	.27	204
TNT	287	1.57	300	2.51 (11)	34.4	5.0	.36	300
PETN	200	1.74	300	6.3 (19)	47.0	6.0	.25	202
TATB	331	1.84	600	3.18 (19)	59.9	10.0		384
DATB	320	1.74	300	1.17 (15)	46.3	6.0	.23	
NQ	200	1.63	500	2.84 (7)	20.9	5.0	.3	
HNS	320	1.65	500	1.53 (9)	30.3	5.0	.4	
H-6		1.76	300	5.12 (11)	31.8	5.3	.3	
Comp B		1.715	300	3.39 (15)	40.9	5.8	.34	
PBXN-107		1.64	500	5.01 (15)	42.	2.7	.30	
PBXN-109		1.68	400	1.023 (14)	36.5	13.0	.34	
PBXN-110		1.67	440	2.68 (19)	51.4	10.	.35	
NC		1.5	500	8.46 (18)	48.5	3.0	.31	
AP/HTPB[a]		1.806	500	1.29 (10)	32.8	12.7	.31	
AP/HTPB[b]		1.715	300	1.35 (8)	27.0	7.5	.29	
Aluminum		2.79				5300.	.21	
Steel		7.89				1000.	.11	
Insulation (typical liner)		1.45				4.0	.2	
glass		2.17				124.	.2	
graphite composite		2.				100 - 1000	.4	
Air (slow cookoff)[c]		0.0007				1.0	.24	
Air (fast cookoff)[c]		0.0005				1.4	.24	
"Foam"		0.1				2.0	.2	

* Lowest experimental values for "a" between 0.003 and 0.039 slab cm thickness.

Numbers in parentheses are powers of ten.

** T_d represents deflagration point or ignition temperature (shown for comparative information only).

[a,b] Typical values for two different (AP/HTPB) reduced smoke composite propellants.

[c] For typical conditions that may occur in thin internal air gaps in the munition system.

HEATING FOLLOWED BY REMOVAL OF HEAT SOURCE

The equations already given should be applicable for a scenario involving heating of a munition for some period of time followed by removal of the heat source or reduction of the heat-source temperature. For this problem it is important that the heat-transfer equations include provision for heat loss from the case to the environment by appropriate mechanisms.

The fast-cookoff spreadsheet method described earlier has been used to examine a heat-removal scenario in which the fire heating term of equation (1-1) was modified subsequent to a particular time step by changing T_f, the flame temperature, to T_a, the ambient temperature. This resulted in either delay of the time-to-ignition or gradual cooling of the charge and complete suppression of ignition, depending predominantly upon the case temperature at the time the heating term was modified. In these limited calculations, using one-second time steps, the transition from continued self heating (and eventual ignition) to cooling with no ignition was very abrupt and one additional second of external heating determined the outcome.

In principle, if the maximum heat content of the system in the scenario minus the heat lost following heat-source removal exceeds the amount of heat required to cause ignition, ignition will occur. On this basis, it should be possible to formulate fairly simple analytical relationships, from data generated by numerical calculations on specific scenarios, to use for predicting additional scenario results for the same munition system.

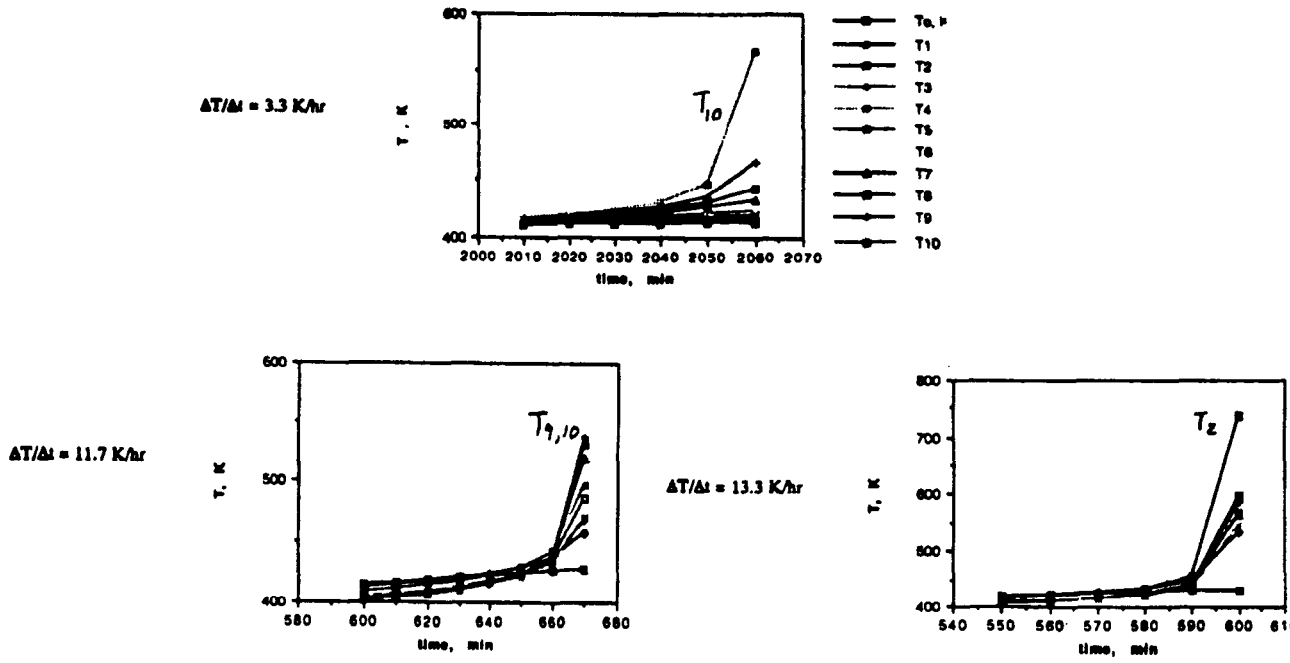

Figure 2-2. Spreadsheet calculated temperature rises for 8-inch Diameter RDX cylinder for slow cookoff heating rates of 3.3K/hr (6°F/hr), 11.67 K/hr, (21°F/hr), and 13.3K/hr (24°F/hr), from spreadsheet calculation.

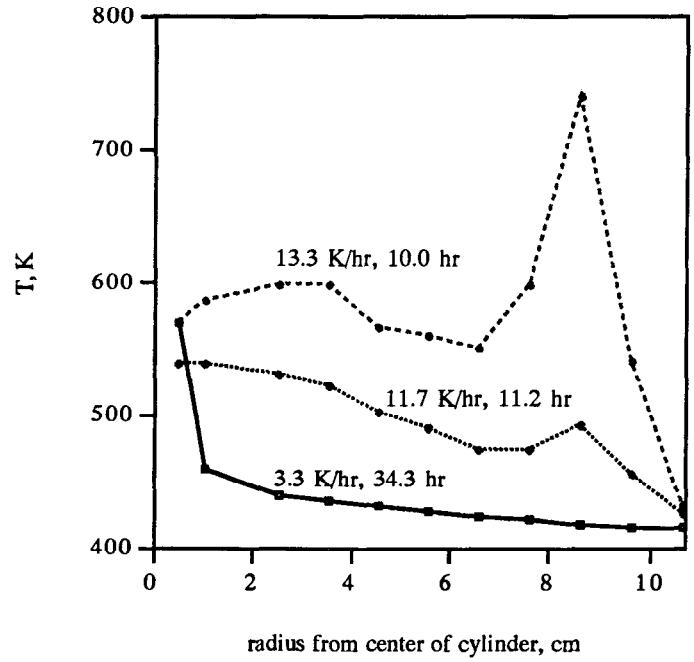

Figure 2-3. Spreadsheet calculated thermal profiles for 8-inch Diameter RDX Cylinder at last time step before ignition for slow cookoff heating rates of 3.3K/hr (6°F/hr), 11.67 K/hr, (21°F/hr), and 13.3K/hr (24°F/hr).

3. INERT MATERIAL BEHAVIOR

Heat transfer calculations for inert components of many munition-system problems can be solved by the methods given in this section. With analytical solutions, the end result of the inert-material calculations should be the physical condition of inert confinement at the time of ignition and the surface-temperature of the contained charge as a function of time. For numerical calculations the complete time history of temperature in inert and energetic components should result.

SPECIAL HEAT TRANSFER SOLUTIONS

Many inert material behaviors were mentioned in Section 2. In this section, these behaviors are organized in a more logical way. At this stage of the heat transfer analysis we will have at least a "first pass" estimate of the temperature-time history of the inert components (T (x, t)). Logical approaches are to organize the inert material behaviors by temperature, by physical result, component, material, by following the heat flow, or by some combination of all. In the following discussion, the last method is chosen as the primary one – that of following the heat flow. In this approach, the materials are traced from those closest to the heat source to those furthest away, typically from the outside inward. The specific components examined are listed below:

a. Outer container wall
   With and without "fire retardant" coating
b. Inner container wall
   With and without insulation
c. Munition case
d. Inner liner
e. Energetic material (see Section 4)

Any errors in calculating the heat transfer rate from the environment to the outer surface of a munition system will cause errors in all parts of the time-to-cookoff calculation. Equation (1-1) is generally applicable to a heat transfer calculation from a flame to any surface submerged in the flame. Equations (2-1) through (2-3) can be applied through successive inner layers of inert materials. If there is no direct flame impingement, heat transfer to the outer surface will generally be due primarily to convection. However a very hot external object near the surface (including a flame) will cause radiative transfer as well, which will be complicated by geometric effects, including field-of-view (FOV) and configuration factors, and will cause unsymmetrical thermal patterns on the surface.

Very resistive materials, such as those used as thermal barriers on munition cases or outer launcher surfaces, require more complicated calculations, even in 1-D analogues. There are several reasons for this: (1) some of the materials, such as intumescent coatings, change dimensions and thermal properties due to application of heat, (2) subliming coatings have a very high effective heat capacity during the sublimation process and may also have decreasing thermal conductivity and density during the process. With such materials, there may be some initial heat conduction to the substrate followed by a period of very little heat conduction while the material is being changed by heating, and finally a period of fairly constant heat transfer through the modified coating material (decreasing as the temperatures equilibrate and increasing as the insulation breaks down). While the thermal behavior of these materials can be modeled in numerical codes, their behavior is more complex than others we have encountered thus far in the protocol. Currently, a number of property values for these materials must be assumed in a numerical model to select those that fit the limited heat transfer data (which usually consists of just a heating rate and backwall temperature-time curve).[9,11] As a simple alternative, the time-temperature curve obtained experimentally (see Figure 3-1 for examples) can be used to define time-temperature values for the substrate (i.e., outer surface of munition or launcher metal case), and the numerical heat transfer calculation can proceed from there. The limitation of this simple approach is that one is limited to data for specific heat transfer rates to the coating-material surface (i.e., specific flame temperatures or experimental arrangements) and a limited number of material thicknesses.

Early stages of heating materials with low thermal conductivity can be modeled with an error function as shown by equation (3-1). The error function approximation is good until the backface temperature rises about 5% of the difference between its initial temperature, T_i, and the temperature of the heated surface, T_S. The error function is plotted in Figure 3-2.

$$(T(x, t) - T_S)/(T_i - T_S) = \text{erf}\,(x/\sqrt{(4\alpha t)}), \text{ where x is distance from surface.} \qquad (3\text{-}1)$$

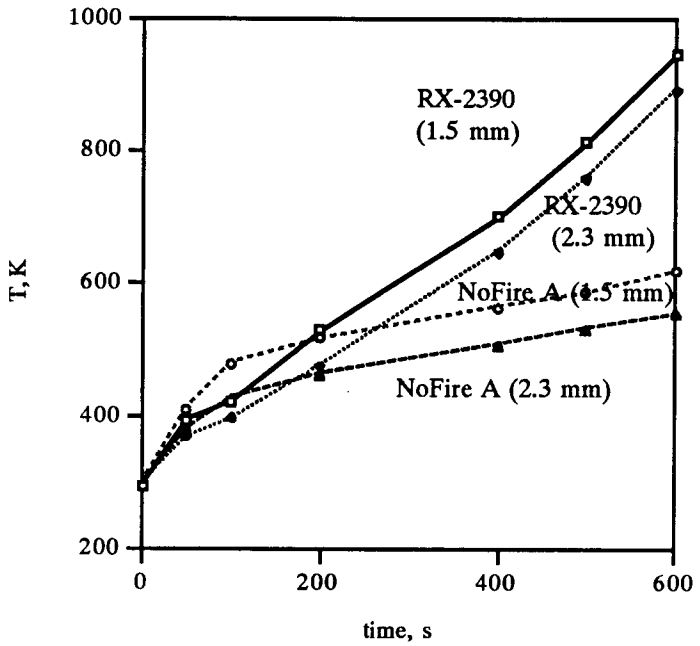

Figure 3-1. Backwall temperature data for two intumescent coating materials: RX-2390 and NoFire A with initial coating thicknesses of 1.5 mm (0.06 inch) and 2.3 mm (0.09 inch) exposed to propane fired oven at 1144 K (1600 °F), adjusted from Koo.[11]

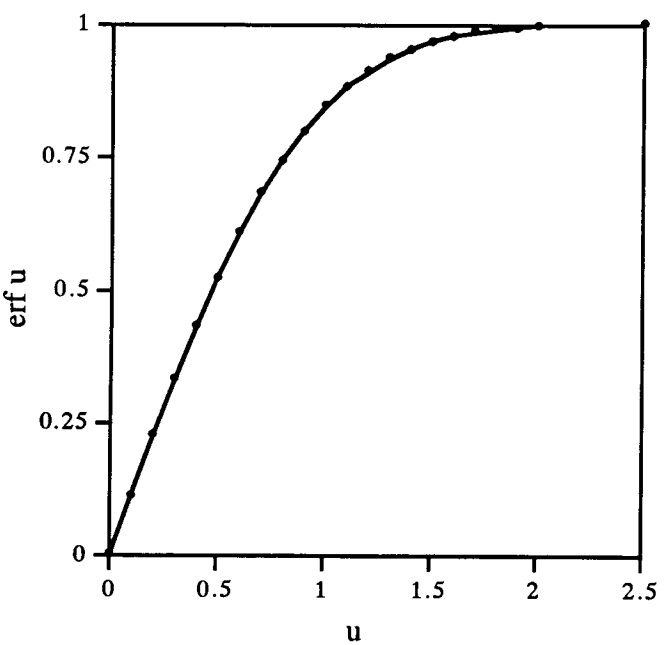

Figure 3-2. Error function, erf u = $(2/\pi)\int_0^u \exp(-u^2)\,du$.

Once heat starts to flow inward from the backwall, equations (2-1) through (2-5) can be used. If the error function is in the function library of an available spreadsheet, in can be used for the early part of the heat transfer calculation in the column that will subsequently contain equation (2-2) for a linearized approximation. Alternatively, the thin insulative surface layer can be divided into a number (that can be estimated by fitting linear steps to Figure 3-2 – also known as Schmidt's graphical method[6]) of grids or shells, perpendicular to the direction of heat flow,

The variation of surface temperature, T_S, convection-heated by an environment at a temperature T_∞ depends strongly on the value of the "thermal inertia," $\lambda^2/\alpha = \lambda\rho C_p$. The surface temperature of materials with low thermal inertia (good insulators) rises quickly when heated as given by equation (3-2) for a surface and environment with convection coefficient, h.

$$(T_s - T_i)/(T_\infty - T_i) = 1 - \exp\,[\alpha t/(\lambda/h)^2]\,(1 - \text{erf}\,[\sqrt{(\alpha t)}/(\lambda/h)] \qquad (3\text{-}2)$$

As with equation (3-1), equation (3-2) applies only while the back surface of the heated medium is unaffected by the heat input at the front surface (i.e., a semi-infinite medium). Equation (3-2) is illustrated for several materials in Figure 3-3. Even though equation (3-2) and Figure 3-3 are for semi-infinite solids, they give some indication of the relative time frames involved in heating solid materials over a range of thermal properties.

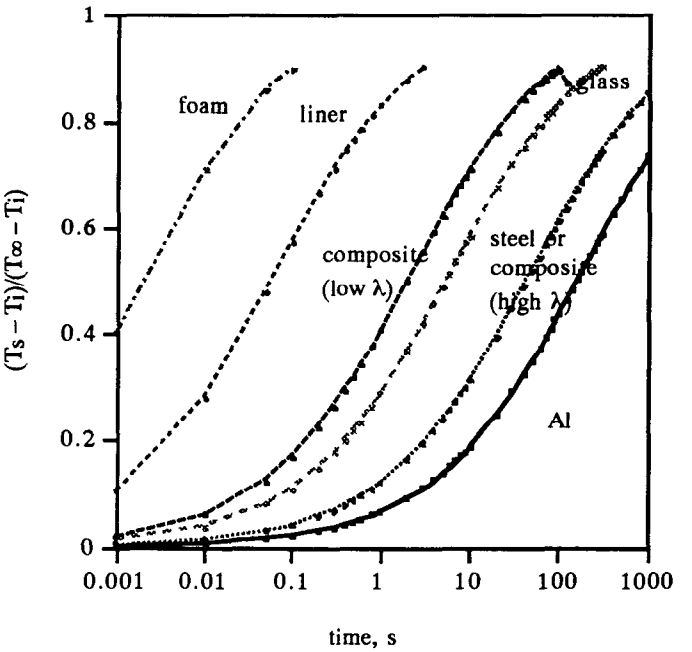

Figure 3-3. Effect of thermal inertia on the rate of temperature rise at the surface of a semi-infinite solid from equation (3-2) and materials in Table 2-1 with h = 0.034 cal/s-cm^2-K.

Once the backface of a layer starts to heat, heat transfer to the next (cooler) layer begins. If the layers are intimately connected, conductive heat transfer equations (2-2) through (2-5) apply. If the inner layers are not in contact, a combination of conduction, convection, and/or radiation through the intervening air or other gaseous medium must be used. The equation for heat transfer by convection to a cylindrical surface of radius r_i is identical to that for conduction across a cylindrical tube of inner and outer radii r_i and r_o, respectively, except that the term $[\ln (r_o/r_i)/\lambda]$ is replaced by the term $[1/r_i\, h)]$. Typically, h takes values in the range 0.005 to 0.05 KW/m^2-K for unforced convection and five times higher for forced convection in air.

Radiation heat transfer is more complicated to calculate. If we limit our consideration to concentric cylinders, Figure 3-4 can be used to determine the configuration factor for radiation transfer between two black body surfaces. If the surfaces are non-black (i.e., gray) the result from Figure 3-4 must be multiplied by the

product of the surface emissivities. In Figure 3-4, $F_{2\text{-}1}$ is the fraction of the energy leaving the outer surface area, A_2, that directly strikes A_1. $F_{2\text{-}2}$ is the fraction of energy leaving area A_2 that does not strike A_1, but directly strikes A_2. For outer cylinders with L/r > 5, as generally applies rather well for many munition-system configurations, it is seen that the configuration factor is almost equal to the radius ratio of the two cylinders, and equation (1-1) may be used with that simple factor. For non-cylindrical outer surfaces, the configuration factor is equal to the surface area ratio of the inner and outer surfaces provided the inner surface is so shaped that it does not receive its own radiation. Radiative heat transfer will be particularly important in flame-heating scenarios. In many cases, important contributions to heat transfer will be made by more than one mechanism.

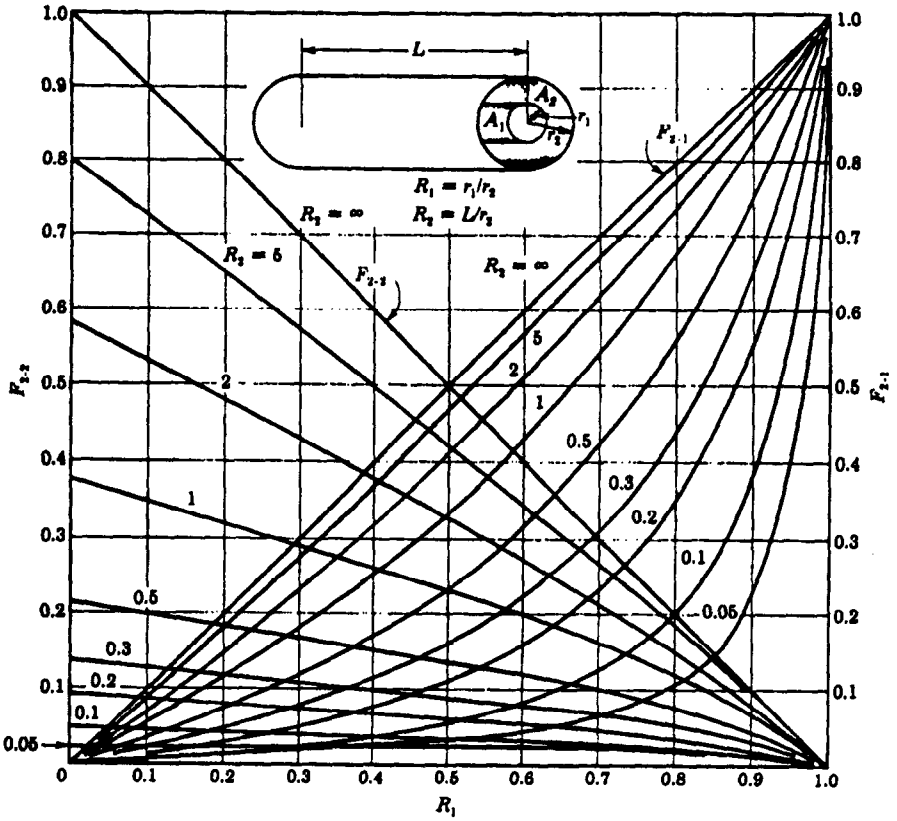

Figure 3-4. Configuration factors for concentric cylinders of finite length.[2]

For heat transfer problems that cannot be calculated directly by straight-forward 1-D models, such as that shown in Figure 3-5, it may still be possible to break the analysis into several 1-D models. Figure 3-5 represents a munition in a container or launcher with different conduction properties at different longitudinal positions. Heat that flows to the munition case through the thinner or more conductive shell (indicated to be of aluminum – which also might melt at high temperatures and expose the munition case to direct flame) will flow both radially into the munition and longitudinally along the munition case. This might be used in a design intended to activate a mildly reacting warhead on the left side of the munition system and to melt a eutectic material (or activate some other mitigation device) in the head end of the rocket motor case to the right side of the system, prior to ignition by radial heat flow through a better insulated portion of the container and into the rocket motor. The calculation will involve radial heat flow as already described and longitudinal (or planar) heat flow along the case area, $A = \pi (r_1^2 - r_2^2)$. This approach has been used successfully to design launcher/munition configurations that reduced rocket motor reaction violence as described two sentences previously.

A similar 2-D heat-transfer problem involves the effect of fins attached to a missile rocket motor. For many years, the US Navy tried to reduce the violence of the Sidewinder rocket motor in fast cookoff tests. Many of the case-opening mitigation concepts now available were originally conceived and tested in the

attempt. All development and testing was done on rocket motors with the fins removed. In final proof-of-concept tests, all concepts – including unmodified motors – were tested with fins in place. Only then was it learned that the fins carried enough heat to the motor case to cause failure and mild burst that resulted in an acceptable burning reaction – with no need for additional mitigation devices.

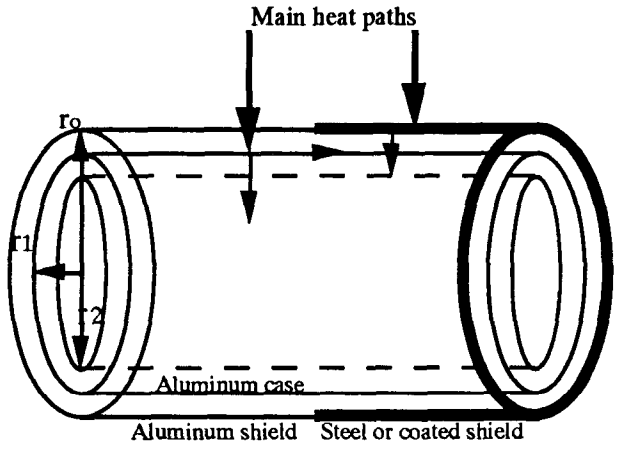

Figure 3-5. Schematic drawing of heat transfer problem involving radial and longitudinal flow.

PHYSICAL CHANGES TO INERT MATERIALS

CONTAINMENT FAILURE

Containers may fail by natural bursting, fragmentation driven by explosion or detonation, failure at weakened locations (as with stress-riser grooves, active or passive mitigation systems[13] or, as indicated above, the gentle assistance of some case attachments), melting, softening, or burning. In high-temperature threat scenarios, the strength of the containment may be reduced naturally as it reaches specific higher temperatures. The driving force that causes initial containment failure may be the result of liner outgassing, EM outgassing, thermal expansion of the heated charge, or burning of the charge – all of which will cause a pressure buildup in a sealed munition. Even in rocket motors with open nozzles, liner outgassing has been observed to cause a pressure buildup in fast-cookoff tests that causes heated-case failure prior to propellant ignition – with simultaneous collapse of center-perforated charges. The ignition of the surface of the charge in fast-cookoff scenarios is delayed by internal coatings on the motor case, and the ignition delay is further enhanced by the increased thermal resistance that accompanies liner outgassing. The quantity of gas generated by outgassing can be estimated as 22,400 cm^3 atm/mole, or typically about 1,000 cm^3 atm/g at one-atmosphere pressure and 273 K. At higher pressures, the volume decreases proportionally to pressure, and at higher temperatures, the volume increases proportionally to T/273. These adjustments do not apply at pressures so high that the ideal gas law fails and molecular co-volumes must be considered, but they should be adequate for case-burst phenomena.

Sealed cases, such as those of many warheads, may burst as the heated charge expands. This failure can be enhanced to occur at lower temperatures (and pressures) by scoring a "stress riser" along the case wall. Such a stress riser must be designed to not interfere with normal operation of the munition and to fail prior to the onset of accelerated burning of the EM (as described in section 5). This means the pressure at which they must be designed to fail will depend on the behavior of the contained EM – particularly for slow cookoff scenarios.

The composite cases being developed for many rocket motors, and epoxy-coated/spiral-wrapped steel-strip-laminate cases fail as pressure vessels in fast-cookoff scenarios, and vent rather benignly, due to their temperature rise and rapid weakening upon direct exposure to flames. Only composite cases containing

polyolefin (Spectra®) fiber have been observed to fail prior to charge ignition in slow-cookoff scenarios as well.[21] The polyolefin fibers also burn in air in fast-cookoff, further enhancing pressure-release failure and mild reaction of the charge.

Aluminum containers, launchers, and munition cases will melt at about 933 K (the exact temperature and behavior depends upon the specific aluminum alloy). In numerical analyses, the latent heat of the failure mechanism should be included in calculations for more accurate time-to-ignition results. Inward heat transfer from the aluminum of a motor or warhead case will delay the temperature rise to melting, and without a sufficient thermal resistance of insulating liner between the aluminum and the EM, ignition will likely precede melting.

OUTGASSING LINERS

In the strictest sense, outgassing liners are not inert, but neither are they "energetic." Several types of outgassing liners have been described: (1) liners containing blowing agents that generate gases at moderately increased temperatures that provide additional thermal resistance between the outer case and the charge surface and (2) liners containing "antioxidants" that combine with free radicals in the decomposing charge that may delay the onset of ignition and/or reduce the speed of subsequent burning and hence reduce the reaction violence.

4. ENERGETIC MATERIALS

ANALYTICAL SOLUTIONS

Equation (2-6) is not solvable in closed form, and it is common practice to solve it for the limiting constant temperature boundary condition, $\partial T_\infty/\partial t = 0$. This defines the critical temperature, T_{cr} in equation (4-1). If the exposure temperature is less than T_{cr}, self-heating ignition will never occur (if the thermal coefficients used truly apply at the boundary condition). Use of single values of E, Q, and Z ignores multiple decomposition reactions that may be occurring and resulting nonlinearity of the slope E as a function of T and heating rate.

$$T_{cr} = E / (R \ln ((a^2 QZEw)/(T_{cr}^2 \alpha C_p \delta R)) \text{, Kelvins, K} \qquad (4\text{-}1)$$

where: a = characteristic dimension; slab half-thickness or cylinder or sphere radius.
δ = shape factor (0.88 for slabs, 2 for cylinders, and 3.32 for spheres).

Note that the unknown variable, T_{cr} appears on both sides of the equation. Equation (4-1) can be quickly solved iteratively on a pocket calculator; it is helpful to note that the left side of the equation is relatively insensitive to the guessed value of T_{cr} on the right side. A 20 K error in T_{cr} on the right side leads to an error of only about 1 K on the left. If an energetic material is exposed to a temperature greater than T_{cr} it will eventually cook off. The time to cookoff at an exposure temperature, T, for a cylinder of energetic material initially at a temperature of 298 K can be approximated with equation (4-2) for $T>T_{cr}$.

$$t_{co} = (\rho C a^2/\lambda) F \qquad (4\text{-}2)$$

where: $F = 10^{\Phi}$

$\Phi = -.008511 - .0173\, v - .0061754\, v^2 + 4.0756 \times 10^{-5}\, v^3$, for a cylinder geometry.

$v = E\,((1/T_{cr}) - (1/T))$, where T is the environmental temperature.

For a sphere, the value of F is about 1/2 as large, and for a slab about 2.5 times larger.

As Creighton astutely observed, an "ignition temperature" that is a function of the heating rate can be specified for an energetic material specimen of a given size and shape subjected to ramped heating (i.e., constant or variable rate).[10] Ignoring transient effects, Creighton derived equation (4-3) to describe the functional dependence of ignition temperature (the surface temperature when runaway reaction begins) of a thickness, a, of a slab of energetic material on the heating rate, β.

$$T_{ign} = E/\{R\,[\ln(pQZ/C_p)] + 1 - \ln\,[(p\beta/(1-(1+p\beta)e^{-p\beta})\,]\,\} \qquad (4\text{-}3)$$

where: $p = E\,a^2/R\,\alpha\,\delta T_s^2$; β = heating rate, K/s ; and $T_{ign} = T_s$ at the solution point.

Creighton used $\delta = 1$, instead of 0.88 for slab, which makes little difference to the value of T_{ign}.

Equation (4-3) bears a strong resemblance to equation (4-1) for critical temperature (particularly, the term p). If the shape factor, $\delta = 2$, is incorporated into the denominator of p in equation (4-3), one might think

offhand it should be applicable for calculating time to cookoff and surface temperature at cookoff for cylindrical munitions. However, as the curves labeled "T_{ign}, K Creighton," in Figure 4-1 show for the AP/HTPB[b] propellant and for HMX explosive, Creighton's curve (with δ applied) is increasingly higher than the spreadsheet calculations for high heating rates and bottoms out too low at low heating rates. There are two obvious reasons for the first problem:

(1) At high heating rates, the characteristic dimension of the problem is no longer the radius of the cylinder, a, but instead is dependent on transient effects as given by the Fourier modulus $Fo = \alpha\, t/a^2$, where α is the thermal diffusivity defined earlier. Therefore, the characteristic dimension becomes $a = \sqrt{(\alpha\, t)}$. This size effect must be accounted for in the spreadsheet calculations by using a sufficiently fine radial grid near the surface – otherwise, the spreadsheet results are incorrect and instead agree quite well with the Creighton curves cited above.

(2) In addition, as the characteristic dimension becomes a thinner and thinner shell on the surface of the cylinder for increasing heating rates, the shape becomes less a cylinder and more a slab. Therefore, the shape factor should gradually change from that for a cylinder, $\delta = 2$ to that for a slab, $\delta = 0.88$.

For the second problem, that of the low value of T_{ign} calculated by equation (4-3) at heating rates characteristic of slow cookoff tests and slower, the only consistent assumption easily adopted is that the activation energy, E, is not perfectly constant over the very wide range of heating rates to which it is here applied, but instead has a systematic variation (that is well within the general reproducibility of reported values). From a more physical standpoint, this variation might be due to the 0^{th} order assumption that fails to account for the decreasing mass fraction of undecomposed energetic material, w in equation (2-6), that may become increasingly important at long heating times, or to the fact that the single value of E used is known to represent an "average" of values for a number of different simultaneous decomposition reactions.

Equation (4-4) results from applying these assumptions and gives the excellent agreement to the spreadsheet calculations as shown in figure 4-1 by the curves labeled "T_{ign} K, mod Creighton" that virtually overlay numerical spreadsheet results for all values of heating rate.

$$T_{ign} = E(\beta) / \{R\,[\ln(p'\,QZ/\,C_p)] + 1 - \ln[(p'\beta/(1-(1+p'\beta)e^{-p'\beta})]\} \qquad (4\text{-}4)$$

where: $p' = E(\beta)\,[a(t)]^2 / R\,\delta(t)\,\alpha\,T_s^2]$

$a(t) = \sqrt{(\alpha t)}$ if $\sqrt{(\alpha t)} < a_o$, otherwise $a(t) = a_o$, the characteristic dimension (radius of the cylinder)

$\delta(t) = \delta_{slab} + (\delta_{cyl} - \delta_{slab})\, a(t) / a_o = 0.88 + (2 - 0.88)\, a(t) / a_o$

$E(\beta) = E_o - 0.032 \log(\beta) + 0.236\,[\log(\beta)]^2$, where E_o is the constant value of activation energy (for $\beta \geq 0.001$, otherwise $E(\beta) = E(0.001)$

$t = (T_s - T_o) / \beta$

There are good physical reasons for these corrections to the characteristic dimension and the shape factor as a simple means to include transient effects in equation (4-4). The correction to activation energy is based only on its success with the two energetic materials shown. Therefore, one should be cautious before extending this method blindly to other energetic materials. However, by comparing this method with the spreadsheet method described earlier for a number of materials, a more extensive data base can be built to explore the generality of the assumption.

Because the solution to equation (4-4) occurs for $T_{ign} = T_s$, the iterative calculation is most easily obtained with a spreadsheet, because of the visibility of the calculation thereon (and its ability to run many situations at one time), or by using iterative logic in a pocket calculator (with memory) for solving one situation at a time. As with T_{cr} in equation (4-1), T_{ign} in equation (4-4) is relatively insensitive to the guessed value of T_s.

The validity of equation (4-4) is further confirmed in Figure 4-2 where calculations for both 2.75-inch and 8-inch diameter rocket motors are compared with cookoff data on rocket motors containing an AP/HTPB propellant measured at heating rates of 6°F/hr (0.000917 K/s) and 75°F/hr (0.011K/s).[1]

For really rapid solutions of fast cookoff in fires, equation (4-5) closely approximates the surface heating rate, β, of energetic materials in cases with the indicated thicknesses of case wall (t_{case} calculated for .17-.4 cm) and internal liner or insulator (t_{liner} calculated for 0-4 cm) for subsequent calculation of ignition temperature and time-to-ignition using equation (4-4). The calculations used to generate equations (4-5) assumed there is no prior heatup time for the ambient flame temperature, and allows the case to heat naturally

under the influence of the opaque flame at T_f K as given by equation (1-1). Initial uniform munition temperature of 294 K was assumed. The equation was based on spreadsheet calculations with λ_{case} between 0.001 and 1.0 cal/cm/sec/K., and T_f between 1033 and 1366 K. For extrapolation to thicker case walls and thicker liners, the linearized equation (4-5a) will give better results (but will fail for cases with no liner). Considering the complexities of the situation it is more surprising that the fast cookoff situation can be fit by curves at all than that there is no general single simple closed form equation.

$$\beta = 1/[0.589(t_{case}\rho_c C_{pc})^{0.9}(1+.0005/\lambda_{case})(1000/T_f)^4 \exp(0.00189\, T_f\, t_{liner}/\,(t_{case})^{0.4})] \quad (4\text{-}5)$$

$$\beta = 1/[(-0.0469 + 0.425\, t_{case}(\rho_c C_{pc}) + (0.846 + 0.921 t_{case}(\rho_c C_{pc})^{0.79})t_{liner}) \times (1+.0005/\lambda_{case})(1033/T_f)^3 \quad (4\text{-}5a)$$

Even without quantitative methods for predicting reaction violence, the ability to predict ignition temperature and time-to-ignition are invaluable tools for selecting eutectic materials and sensor activation temperatures for the design of case-venting of early-ignition mitigation systems, and thermal shield designs for delaying ignition in specific scenarios. The main advantage to be gained by more sophisticated two- and three-dimensional thermal models may be to explore fine design details of irregular shapes, and to explore even lower heating rates (although numerical stiffness problems interfere), heat source removal problems, or constant temperature boundary conditions that are used in some small-scale tests.

PHYSICAL AND CHEMICAL CHANGES

Heated energetic materials may undergo physical and chemical changes during heating prior to auto-ignition. Changes that have been observed include liquification, gas generation, foaming (i.e., internal void formation), softening, and even hardening. Some of these changes will cause the burning behavior of an EM to change drastically, even if it is not heated to auto-ignition, but ignited at some specific temperature instead.[12]

For AP/HTPB propellants, the soak temperature (8 hours) at which burning transitions to explosive violence, in rocket motor cases, has been determined to be between 422 and 435 K.[12] In general, this is in the vicinity of the temperature at which propellant foaming has been observed in small, heated samples.[1] The unconfined burning, due to auto-ignition, of such materials is not particularly violent, but when confined for more than a millisecond following ignition, very violent explosions often occur. There appears to be some coupling between changes in EM mechanical properties at higher temperatures, void formation, and the violence of the ensuing reaction that occurs in slow cookoff of confined charges. These factors are accounted for in the simple model described in Section 5.

Thermal expansion of the charge may burst the case or loosen end closures in sealed warheads. This effect is further enhanced by charge and liner outgassing. When coupled with a case-weakening groove ("stress riser") the case may be passively vented to prevent violent reaction.

Changes in EM mechanical properties when heated undoubtedly have significant effects on burning behavior as pressure rises. It is therefore important that these changes be determined for each EM in a munition system and applied to calculations of reaction violence.

Seemingly small differences in EM formulation (type of binder, curing agent, burn rate catalyst, choice of plasticizer, and presence or absence of other ingredients) have been found to dramatically affect the physical, chemical, ignition, and burning (cookoff) behavior of energetic materials.[1]

Clearly, there is some region of heating rates where the behavior of a munition transitions from its "slow cookoff" behavior to its "fast cookoff" behavior. This region is not usually sought in testing, and has only rarely been the subject of analysis. Perhaps it is associated with a specific value of the Fourier modulus, $Fo = \alpha\, t/a^2$ to the extent that the ignition point moves from the surface to the interior of the munition as the heating rate decreases and the time-to-cookoff increases. Limited data indicate that for a given energetic material and heating rate, larger munitions may cookoff less violently than smaller. However, for a specific munition, the distinction between fast and slow-cookoff behavior will also depend on heat transfer and mechanical behavior of the outer inert components, particularly at higher heating rates. Figure 2-3 shows the ignition point of RDX moving from the center toward the outer surface with increasing heating rate. The larger the critical dimension, a, of a munition, the lower its critical temperature, T_{cr}, and the shorter the time to autoignition in "slow-cookoff" scenarios (although this effect is most pronounced at the smallest sizes). Using Figure 4-2 as an example, we see that for the AP/HTPB charge in 2.75-inch (7 cm) and 8-inch (20.3 cm) diameter rocket motors, this transition in the larger charge appears to begin at a heating rate of about 0.005 K/s (32°F/hr).

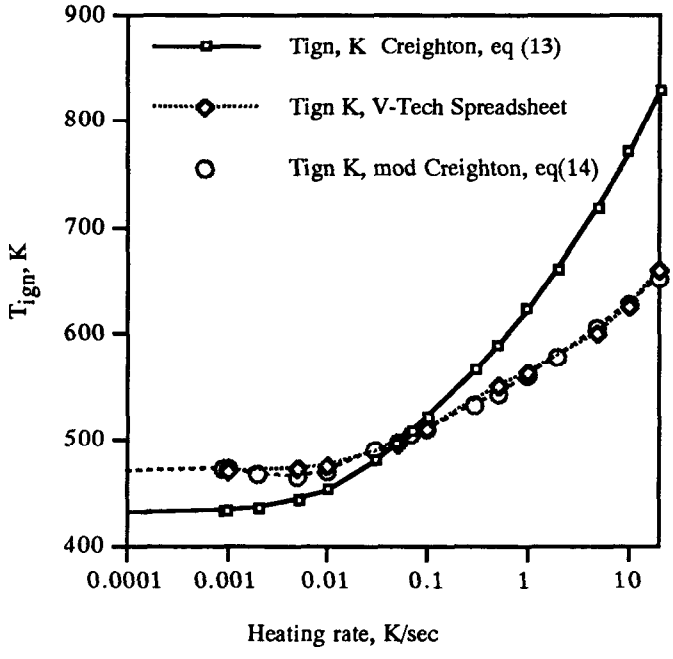

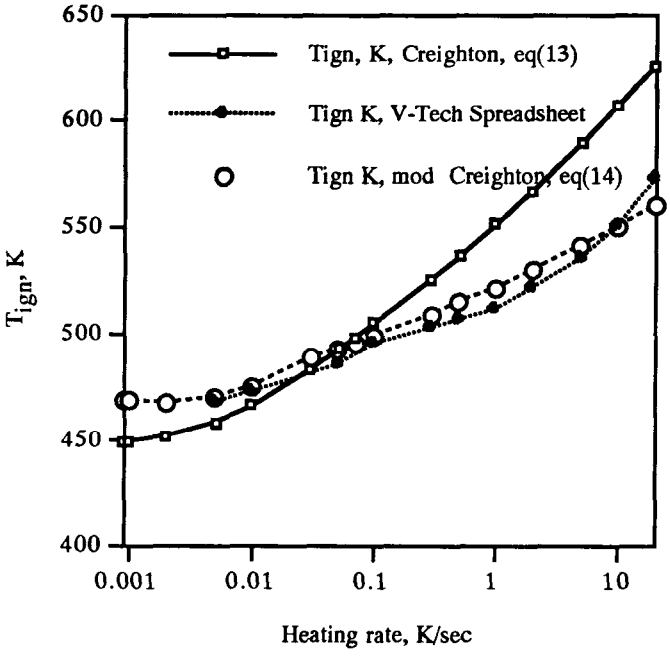

Figure 4-1. Comparison of spreadsheet and algebraic cookoff calculations (a ~ 3.2 cm for both materials).

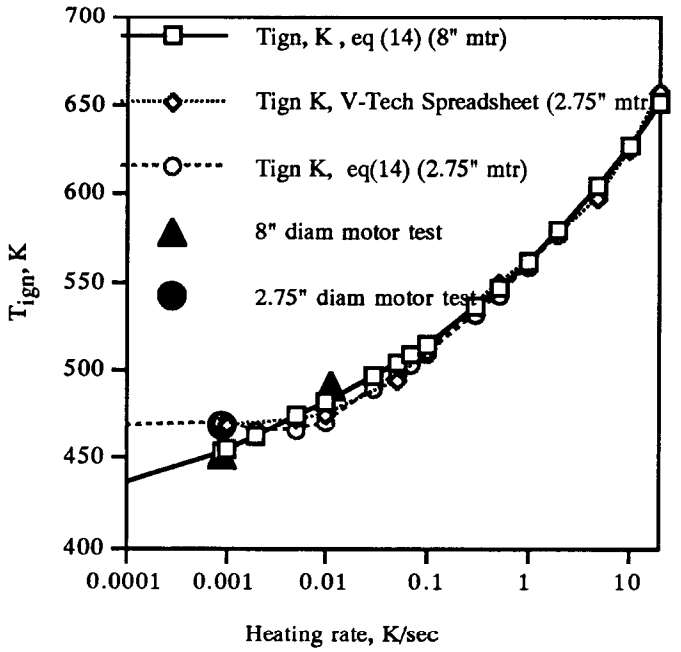

Figure 4-2. Comparison of analytical cookoff calculations with data.

SELF-HEATING OF ENERGETIC MATERIAL

The self heating calculations for energetic materials have already been described by equations given in Section 2 and earlier in this section. These calculations take the munition to the point of ignition. There is also the possibility that the heating profile in a particular munition test or threat scenario will be so different from the conditions at which the important parameters (Z, E, and Q) have been derived from measurements that the measured parameters will not accurately apply.

Another problem is that heat-transfer and self-heating calculations can usually be made assuming zero-order kinetics (that is, the fraction of material decomposed, given by w in equation (4-1) and neglected elsewhere in this protocol, can be ignored). This may result in serious errors, particularly for extensive exposure to relatively low temperatures – near the critical temperature [equation (4-1)] – because significant changes to the EM may occur that invalidate the measured parameters.

IGNITION

Ignition is found "automatically" for most EMs in most numerical codes (including the spreadsheet codes) by an "explosive" rate of temperature rise.[8] The values thus determined for time-to-ignition and temperature of the surface of the munition at ignition have agreed very well with measured values for a number of munitions and EMs. These values agree with those given by equation (4-4) for those EMs that have been compared. This method of calculation has also given reasonable values for ignition in projectile-impact scenarios assuming a shear-heating mechanism (see Section 13 of the NIMIC Bullet/Fragment Impact Protocol).

5. BURN

Following ignition after heating at slow to moderate rates, some EMs have been observed to detonate in quite small samples with no confining case. A brief discussion of a possible mechanism is given later in this section.

Many EMs, when unconfined, burn following ignition, after being heated at all rates that have been studied. Some burn more violently than others (consumption of 500 grams may take from a fraction of a second to several minutes), and the overpressure due the generation of gas at the shortest burn times causes some local damage to test ovens. When the burning EM is confined (as in a munition case), the rising pressure due to confined product gas, accelerates the linear burning rate. If the gas generation rate within the confinement exceeds the rate of gas loss through nozzles, vents, or other openings, the pressure rise may continue until either (1) the EM is fully consumed, (2) the case bursts, or (3) the burning reaction transitions to a detonation (which of course will fragment the case).

Two case burst modes, due to pressure rise, have been observed. One is fairly mild, usually evidenced by splitting of the case into two or three pieces at a pressure near the static yield strength of the case (either hoop failure or separation of end covers). Presumably, this case failure is due to fairly slowly rising internal pressure.

The other failure mode must be termed explosive, although it is often ranked a "burn" or "deflagration" depending on whether case debris is propelled less than or more than 15 meters. The case may fragment into many pieces, but there is no evidence of the many very small fragments and plastic failure typical of a detonation. Blast overpressures at significant distances from the munition are usually measurable. Presumably this case failure is due to very rapidly rising internal pressure. The distances to which debris is thrown often correlates analytically with internal pressure values significantly higher than the static yield strength of the case.

The mild burning is explained by burning in the "normal mode" typical of a rocket motor. In this case, the burning surface regression is controlled, sometimes referred to as "burning in parallel layers."[14] If the charge is fully confined or sufficiently confined that openings will choke the exiting gases and cause supersonic exhaust gas flow, equation (5-1) may be used to define the pressure buildup.

$$dP/dt = ((dm/dt)_b - (dm/dt)_v)\, R\, T / MV \qquad (5\text{-}1)$$

where:

M = average molecular weight of the product gas

V = free gas volume within case, which increases with time as $dV/dt = dm/dt_{(produced)} / \rho_p$
free gas volume will also increase with pressure and time due to compression of voids in charge

P = internal pressure in case

T = temperature of combustion products within case

R = gas constant,

$(dm/dt)_b$ = mass production rate at burning surface $(A_b) \sim K \cdot A_b\, \rho_p\, P^n$

$$(dm/dt)_v = A_t\, P\, k \sqrt{\{[2/(k+1)]^{(k+1)/(k-1)}\}} / \sqrt{(kRT)} \qquad (5\text{-}1a)$$

$(dm/dt)_v$ = mass flow rate from vents

A_t = vent area, R = gas constant, K = a constant ρ_p = propellant density

k = ratio of specific heats of product gas, typically about 1.2

There is evidence that in equation (5-1), although the exponent n is constant for many EMs over a wide range of pressure, it will show increases at higher pressures [greater than about 20 MPa (3,000 psi) for many propellants]. Also, the burning rate tends to increase with increased bulk temperature of the EM. These factors should be accounted for in using equation (5-1) for cookoff calculations. Using equation (5-1) for a sealed container (i.e., no vent) results in curves much like those to the right side of Figure 5-1.

The three curves to the left side of Figure 5-1 may be considered to be representative of "accelerated burning." The major phenomena to be modeled appear to be:

[1] Heating phase culminating in terminal thermal profile and ignition (Sections 2 & 4),
[2] Initial burning phase accompanied by relatively slow pressure rise,
[3] Transition phase, where the critical pressure, P_{tr}, or critical pressure rise rate, $(dP/dt)_{cr}$, for transition to accelerated burning (due to increased surface area) is reached,[27]
[4] Accelerated burning phase, during which very rapid pressure rise occurs,
[5] Transition to detonation (if it occurs),
[6] Case failure,
[7] Termination of the reaction event.

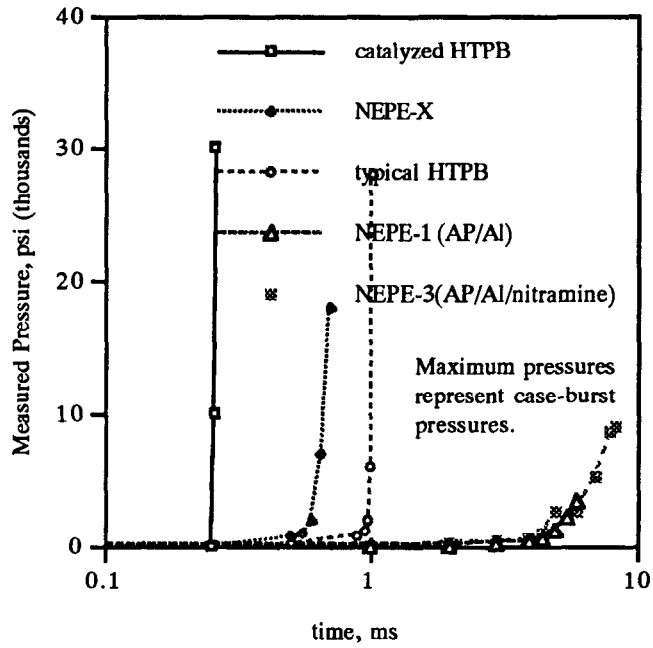

Figure 5-1. Examples of rapid pressure rise measured in slow-cookoff tests by Butcher.[15] Pressure rise rates at 3000 psi: catalyzed HTPB, 5 GPa/ms; typical HTPB, 1.8 GPa/ms; NEPE-1, 0.019 GPa/ms.[16]

Some energetic materials (EM) experience only a limited number of these phenomena; for example, NEPE-1 and -3 propellants in Figure 5-1 appear to undergo only steps [1], [2], [6], and [7]. The other propellants in Figure 5-1 appear to experience also steps [3] and [4]. For step [5] to occur, there must be a sufficient "depth" of EM for the pressure growth to reach a pressure level at which shock initiation of the remaining thermally damaged EM occurs.[18] The phenomenological steps are shown in the flowchart of Figure 5-2.

To modify equation (5-1) for slow cookoff violence, the laminar (or 1-dimensional) burning rate of the energetic material should be modified to account for temperature, pressure, and time effects as indicated by equation (5-2).

$$(dm/dt)_b \sim K(T_p)\, A_b(P, t)\, \rho_p\, P^{n(T, P)} \qquad (5\text{-}2)$$

where: $A_b(P, t) = A_{bo}\, a\, e^{b(t-to)}$ for $P>P_{tr}$ and $= A_{bo}$ for $P<P_{tr}$

P_{tr} = pressure for transition to convective or "mass" burning $= \int_o^{to} (dP/dt)\, dt$.

If there is evidence that EM ignition occurs on an exposed surface (for example, in an SCV [slow cookoff visualization] test),[1] A_{bo} may be set equal to the area of an appropriate surface in the munition. However, if EM ignition occurs within the charge volume, selecting a value for A_{bo} is problematic, and its value will continually increase during the slow burning phase, [2], until the transition phase is reached. If ignition starts on the internal surface of a void, the internal pressure will quickly increase to the situation at which each gram of EM generates about 10,000 cm^3 gas (atmospheric pressure and 3000 K, assuming ideal gas behavior) or over 1 GPa of pressure at constant volume. If internal ignition is assumed to start at a geometric point and grow radially, as a sphere, the conversion of solid EM to hot combustion product gases will "immediately" generate pressures of order > 1 GPa, probably sufficiently high to generate a shock wave for "instantaneous" transition to detonation in many heat-damaged EMs (see below). At such conditions, the ideal gas law is invalid and conditions similar to those for shock-wave propagation and hot-spot ignition in SDT initiation may apply.

We usually have no knowledge of the exact location of ignition in most slow cookoff tests that are performed in sealed ovens. On some occasions, video cameras within the ovens have recorded exudation of

EM from the munition, ignition outside the munition, and propagation of the flame into the munition followed by a violent reaction.[17] SCV tests have occasionally shown surface ignition of propellants even when the interior showed higher temperatures as evidence of internal self-heating.

The pressure, P_{tr}, at which the transition to accelerated burning begins depends upon the mechanical properties of the heated, damaged EM in a manner as yet undefined. However, several factors are clear from Figure 5-1: (1) the relevant strain occurs at a high rate of changing stress, (2) the deformation occurs in compression or a combination of compression and shear, (3) the deformation is rapid. When P_{tr} is reached, the EM may have yielded sufficiently to create initial inter-connected porosity and flame penetration (or this condition is created upon reaching P_{tr}). Kuo and Kooker suggest that flame penetration into charges, that causes crack branching at ambient temperature, requires pressure gradients that can be related to pressure rise rates greater than 17.5 GPa/s. If this is also the case in heat-damaged propellants in slow cookoff, one would expect to find lower values of P_{tr} corresponding to higher propellant laminar burn rates. Charge confinement and munition dimensions may be such as to prevent the pressure at the burning surface from reaching P_{tr}. In that case, the transition will not occur and the combustion reaction will continue fairly mildly to completion. (Evidence for this has been found in slow cookoff tests of PBXN-107 containing submunition warheads within an aluminum warhead case with a stress-riser failure strength of about 5.5 MPa (800 psi). Without the stress-riser, more violent reactions occurred. Yet the warhead design was such that only burning explosive, and not thermal expansion, could have fractured the case. This is the reason adequate venting effectively mitigates slow cookoff violence. For a stress riser to prevent a violent reaction, it must prevent the pressure at the burning region from achieving P_{tr}. Once P_{tr} is reached, it is possible for subsequent rapid pressure buildup to greatly exceed the static strength of the confinement prior to case burst.

As the pressure rises, a shock wave may form and propagate supersonically into the unreacted EM. If the SDT initiation pressure of the EM is exceeded and there is enough remaining EM, a transition to detonation can occur. This is the deflagration-to-detonation transition (DDT). Although Sandusky reports SDT in porous beds at sustained pressures as low as 0.1 GPa (14,5[illegible] psi),[18] achievement of rapidly rising pressures about 1 GPa may be a better criterion for DDT.

The munition case will burst after experiencing internal pressure greater than its yield strength. If the case has been vented prior to ignition, it may experience no additional deformation, or perhaps at most only slight additional opening (characteristic of applied internal pressure no greater than 2-5 atmospheres), based on test results and correlation with stress analysis. If the case vents during the slow pressure buildup phase, [2], transition to accelerated burning may be prevented if the reduced pressure reaches the burning surface before the transition; this depends upon the munition dimensions and geometry and the relative locations of the vent and the burning region. If the transition to accelerated burning occurs, [3] – [4], the case will experience a rapid pressure rise and burst a short time later with an internal pressure in the burning region as given by equation (7-1). If the munition is sufficiently large, and the pressure buildup fast enough, a DDT may occur and the case debris will show evidence of a detonation. All these phenomena have been observed in subscale and/or full-scale tests of rocket motors containing AP/HTPB propellant.[1,12,18]

From equation (5-1), one can see that A_b must increase rapidly (assuming the exponent, n, of P remains constant) to generate an explosive response (i.e., dp/dt ≥ 1 GPa/ms) as shown in Figure 5-1. If this happens, it can make little difference if a long, small-diameter cylindrical motor case is vented at both ends. The results of several calculations with equation (5-1) are shown in Figure 5-3. In these calculations, the dimensions and EM mass of the test were taken from Butcher's paper and the vessel was assumed to be sealed, as in Butcher's experiments (i.e., A_t = 0), with free volume or ullage of 7 cm^3. The Kuo-Kooker $(dP/dt)_{cr} \geq 17.5$ GPa/s criterion was used to start accelerated burning.[27] For the "non-explosive" example (based on $r_b = 0.1\ P^{.5}$), which reproduces the data for propellants NEPE-1 and NEPE-3 quite well, the burning surface of the propellant sample holds constant throughout the calculation because $(dP/dt)_{cr} \geq 17.5$ GPa/s is not reached at pressures less than the burst pressure of the test bomb. To simulate accelerated burning in damaged or foamed propellant, the burning surface was increased exponentially by multiplying A_b from the previous step by 1.5 in each calculational time step (Δt =.01 ms) after the Kuo-Kooker criterion was reached. In these calculations, surface burning alone (at the lowest r_b examined) is sufficient to burst a pressure vessel mildly within 6-8 ms of ignition. The more explosive, very rapid pressure rises require that additional burning area become involved at an increasingly rapid rate (values of the multiplier between 1.1 and 2.0 were examined, and the dp/dt slope is clearly a function of both r_b and the multiplier of A_b, but only results with a multiplier of 1.5 are shown in Figure 5-3 to avoid unnecessary complexity). The time after ignition at which burst occurs is a function of the pressure at which burning rate acceleration is calculated to commence, the

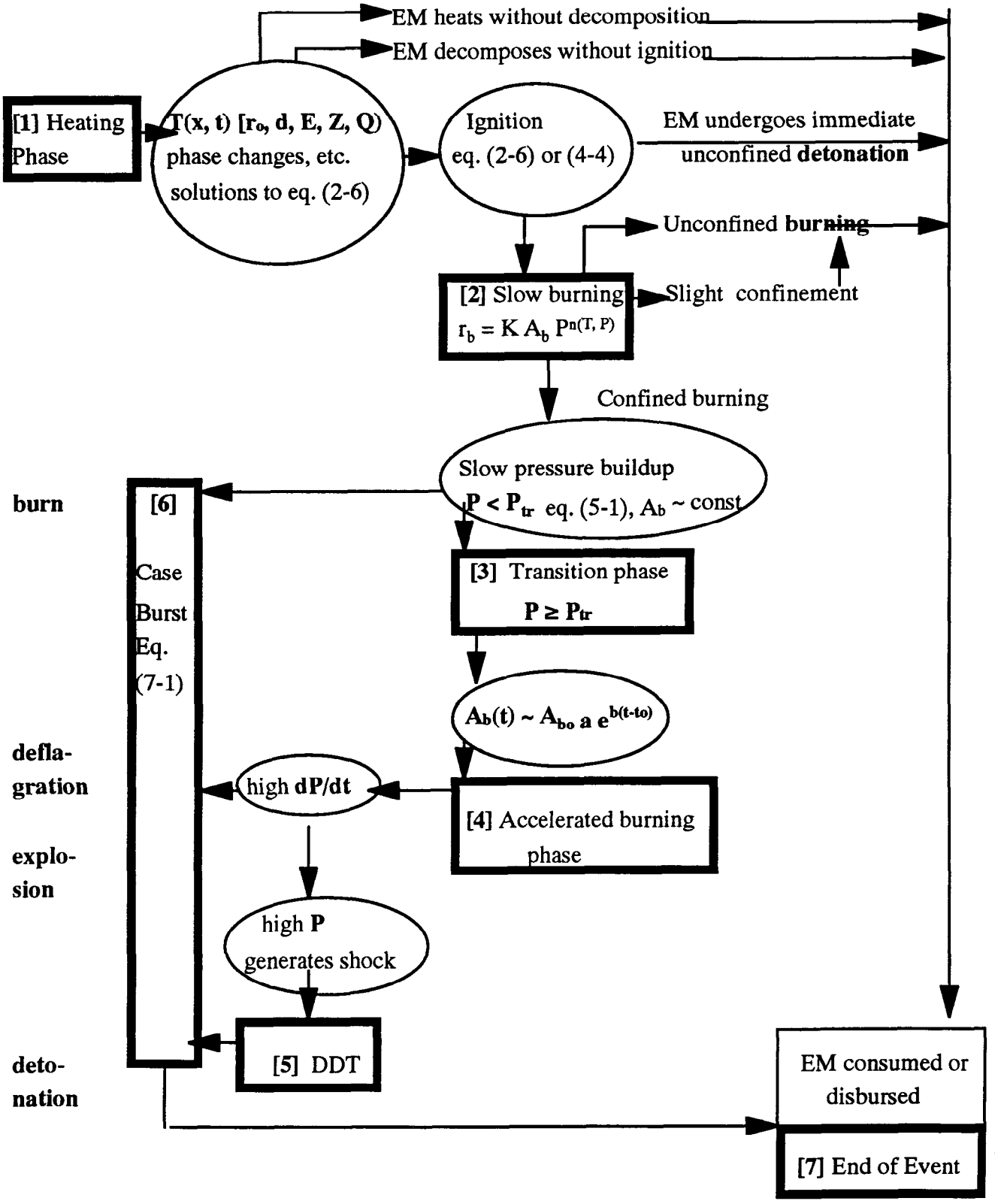

Figure 5-2. Schematic flowchart of slow cookoff reaction violence events characteristic of AP/HTPB

coefficients in the burning rate equation, the ullage volume above the propellant surface, the total volume of the propellant, the volume fraction of voids in the propellant, and the yield strength of the porous propellant.

While this calculational success does not give us an a priori prediction method for reaction violence in slow cookoff, it does – when combined with equation (7-1) – show the "shape" of simple prediction methods we can expect to be derived in the future for situations typical of AP/HTPB propellant rocket motors. It also gives indication of the critical measured parameters that would be required as input for such predictive methods. Test calculations showed that although increasing the value of n from 0.5 (as used in all the calculations) to 1.0, but holding A_b constant, increased the calculated pressure rise rate, it came nowhere near reproducing the rates measured by Butcher.

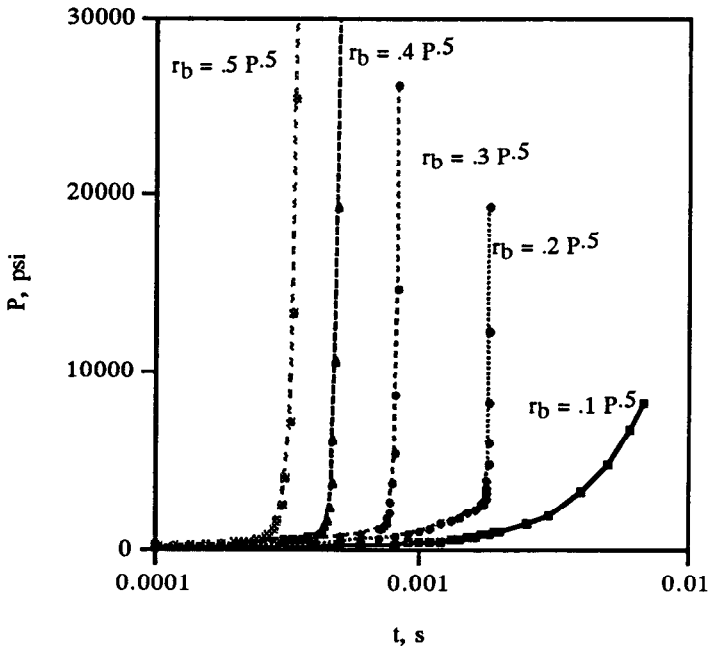

Figure 5-3. Calculations with equation (5-1) assuming a sealed vessel ($(dm/dt)_v$ = 0) closely simulate Butcher's measuerd P(t) results shown in Figure 5-1. Several basic propellant burn rates were used. To simulate rapid pressure rise, the burning surface area, A_b, was assumed to increase by a factor of 1.5 for each time step (Δt= .01 ms) assuming the criterion[27] that convective burning starts when dP/dt reaches 1.75 x 10^{10} Pa/s. Effects of compression of voids in the propellant on increasing ullage volume during burning were ignored. P is in atmospheres, r_b in cm/s.

A number of important factors have been ignored in these preliminary calculations including the temperature dependence of burning rate and the dependence of the pressure exponent, n, on pressure.[7,19] These can be readily included if they are known, however, with no knowledge of values of these factors for the propellants in the database, there seemed to be little point in adding additional variables to the speculative calculations. Even with these other factors considered, it seems clear that a burning process, requiring rapidly increasing burning surface area, is the critical factor in many explosive responses to slow-cookoff tests. Since there is compelling evidence that many such burns are preceded by foaming of the energetic material,[1] there is at least a qualitative basis for such behavior. The behavior observed in Butcher's slow cookoff bomb tests and described above is consistent with theories of accelerating burning that are applied to pre-DDT phenomena in cracked or granular propellants.[27] It is extremely important to remain aware that many energetic materials react violently to slow heating without any ullage in the container or apparent foaming of the material. This behavior is not explained by the preceding model.

At this time, the tests required to determine energetic material properties related to the phenomena described in this section are not performed (or even defined). It seems clear, that mechanical condition and properties of energetic materials at elevated temperature (just prior to self ignition) are required, and some

correlation between these properties and burning behavior at high pressures must be known. The SCV test[1] provides limited information on porosity, and by the use of penetrometers – viscosity or stress/strain at ambient pressure. The presence of fairly uniform porosity is a clear indication that the energetic material matrix retains sufficient strength to support its own weight. Actual tensile-strength measurements on material samples would be difficult and hazardous to make at these conditions, and might give ambiguous results.

PROPULSIVE BURNING

Equation (5-1a) is the equation for mass flow from a choked (i.e., supersonic) nozzle, and is related to the propulsive thrust (force) that will result if burning proceeds within the vented enclosure, given by equation (5-3).

$$F = I_{sp} (dm/dt)_v \qquad (5\text{-}3)$$

where:

I_{sp} = EM specific impulse, N/kg-s, adjusted for burning pressure and nozzle (vent) shape.

I_{sp} is often defined as $lb_f/lb_m/s$ by US propellant developers or as N-s/kg·g_o where $g_o = 9.8\ m/s^2$ and thus described in units of "seconds." In units of seconds, Isp is typically between 150 and 250s – and to use it thus in equation (5-3) divide by the appropriate value of g_o. Isp will be lower at low combustion pressures and higher at high pressures.

6. PRESSURE BUILDUP

As shown in Section 5, the pressure buildup cannot be separated from the burning process. Nevertheless, in any model, as transition regions are reached, it is often necessary to change the calculation. This was shown for the transition from "controlled" to "accelerated" burning when the transition pressure, P_{tr}, was reached.

A similar change will be required when the pressure region, P_{DDT}, accompanying a deflagration-to-detonation transition (DDT) is reached. At P_{DDT} the model will require generation of a shock wave and propagation of this shock into the thermally degraded EM. The nature of such models is not treated here, but it is the subject of extensive on-going research.[18,20,27]

The initial rate of pressure buildup will be strongly dependent on the ratio of the burning surface area, A_b, to the initial ullage (free) volume above the burning surface. The greater the free volume, the slower the pressure rise rate for a given A_b. The free volume will increase during the burn due, obviously, to propellant burnback (as indicated in equation (5-1)).

Another factor that will tend to increase the rate of growth of the free volume, and thus reduce the pressure rise rate, is compression of voids in a foamed energetic material. This is not a trivial calculation, since the increasingly higher pressure waves will travel continuously into the energetic material at sonic velocity. Sonic velocity will increase as the void volume decreases. The instantaneous pressure, and thus the amount of void compression, will always be greatest (at any instant) in the matrix near the burning surface.

In slow-cookoff tests, the entire matrix will be very close to the ignition temperature, T_{ign}, as given by equation (4-4). Any strength remaining in the matrix at this temperature will tend to resist compression of the voids until the burn-generated pressure exceeds the yield strength of the matrix.

Although the influence of these factors was examined in calculations for the study that supported preparation of this protocol, no formal analytical method involving all these factors was developed.

Because the entire matrix is so close to T_{ign}, it is possible that accelerated burning is propagated by heating due to void compression occurring behind a pressure wave of some intensity. This could be tested by pressure measurements, similar to Butcher's,[15] in a bomb test involving intentional ignition of a propellant soaked to different initial temperatures, in a manner similar to the tests of Magnum, et al.[12] If the time delay to accelerated burning is found to depend on the soak temperature, but the succeeding pressure rise rate is relatively independent of soak temperature, this would lend support to this mechanism.

7. EXPLOSION

The resulting reaction will be an "explosion" if the pressure in the reacting EM significantly exceeds the burst strength of the case. In this case, the internal pressure on the burst case and EM fragments will create debris trajectories of significant range.

To a rough approximation, the effective maximum internal pressure at case burst appears to be estimated by equation (7-1). This gives results in reasonable agreement with Butcher's data,[15] and consistent with experience in full-scale slow cookoff tests.

$$P\ (\text{burst}) = (a/c)\ dp/dt + P_{\text{static burst}} \qquad (7\text{-}1)$$

where a is a critical dimension (i.e., radius of test item); c is the velocity of sound in the material within the test item; dp/dt is the pressure rise rate (although perhaps dp(t)/dt should be used) at the case static-burst pressure, $P_{\text{static burst}}$. When subjected to very rapid pressure rises, the effective dynamic response of the case may be estimated from its dynamic yield strength (approximately 140,000 psi for aluminum and 350,000 to 700,000 psi for steels), rather than the lower static values, and verified to some extent by measured debris velocities and trajectories.

The reasoning behind equation (7-1) is that the pressure rise is so rapid that it continues to accelerate before the pressure wave (assumed to be at a pressure equal to the case strength) reaches the case (travelling a distance, a, at sonic velocity, c). During the time the wave is traveling toward the case, the combustion pressure is assumed to continue to rise at a constant dp/dt (although, in Butcher's examples[15] and in equation (5-1) or (5-2) dp/dt continues to increase).

Explosive responses in fast cookoff tests are often seen with AP/HTPB propellant rocket motors. Usually, these might better be called "deflagrations" when the case is broken into a few fairly large pieces, and burning chunks of propellant are thrown further than 15 meters. In reactions such as these, it is not clear how large a pressure has accelerated the debris, but it appears to be significantly greater than the case-burst pressure, and has produced measureable air shocks. Providing for a case-burst prior to EM ignition will usually eliminate most explosive responses.

Reasonable estimates of the internal pressure in an explosion can be obtained from debris velocities or maximum debris trajectory range (as a function of debris shape and size – i.e., mass and drag), using simple kinematic calculations and from blast overpressure data – using Kinney's method given in equation (7-2).[24,25] Kinney's method generates values for energy of explosion from the internal pressure and volume of the bursting vessel. These values of energy are compared to the energy in TNT explosive to obtain an equivalent weight of detonating TNT. Baker's more complicated method gives values of burst energy that are the same as Kinney's at high vessel pressures (> 4000 psia) but slightly lower at lower pressures.[26] Kinney's method, as given by equation (7-2) is more widely used, reportedly with success for both gas-filled pressure-bottle bursts and non-detonating explosions due to combustion of energetic material contained in a vessel. Equation (7-2) ignores the effects of energy transfer to debris. The effects of afterburning subsequent to burst would be calculated by another method.[25]

$$E = [PV/(k\text{-}1)]\ [1 - (P_a/P)^{(k-1)/k}] \qquad (7\text{-}2)$$

$$EW = E/(4.610 \times 10^6)\text{, explosive yield in TNT equivalents, kg; with E in joules.}$$

where

E = energy of explosion in consistent units
V = volume of the exploding vessel at absolute pressure, P
P_a = ambient pressure into which the gas expands
k = heat capacity ratio for the gas

8. DEFLAGRATION-TO-DETONATION TRANSITION (DDT)

For the level of this protocol, no better guide to estimating a DDT can be given than that if the pressure in a confined, burning energetic material shows continuous acceleration as in Figures 5-1 and 5-3, and if there is sufficient depth of energetic material for the rapidly rising pressure in a slow cookoff reaction to reach about 1 GPa (or a different value determined from experiments on heated EM), a transition to detonation is a distinct possibility. Whether or not this transition will actually occur depends upon the detonation properties of the heated EM.

DETONATION

Detonation can occur as the result of a DDT, outlined by the progression described in Sections 5, 6, and 7.

As mentioned in earlier sections of this protocol, detonations have also been observed in unconfined EMs, specifically and surprisingly, in slow and moderate-rate (3.3 K/hr, 14 K/hr and 42 K/hr) cookoff tests of rocket propellants containing AP, poly (1,2-butylene) glycol, and copper chromite catalyst. In these specific propellants, volumetric expansion prior to ignition did or didn't occur depending upon the specific formulations. No mechanism for the detonations has been proposed. Study of these propellants in Butcher's test[15] might give some indication of the promptness of pressure rise and hence of the mechanism(s) leading to detonation. It is possible that the copper chromite so sensitizes the propellant that it transitions to detonation upon the rapid pressure rise of internal ignition at a very small site (as described immediately following equation (5-2)). It is also possible that the copper chromite causes microscopic regions of decomposition that ignite internally leading to very rapid confined pressure rise as described in section 5.

9. END OF THERMAL EVENT

The thermal event is considered to be complete after all EM reactions have ceased. This may occur in a number of ways.

NO IGNITION

If there is little or no self heating of the munition, decomposition may go to completion without ignition. This has not been the case with any of the energetic materials examined in IM programs. Another possibility is that decomposition does not occur, and hence no reaction.

BURNING

A number of paths for burning reactions are given in this protocol. For quiescent burning, the thermal event ends when all EM is consumed or extinguished. Most energetic material will burn within 15 meters of the test item and no debris constitutes a "hazardous fragment" beyond 15 meters. Thrown EM debris (from more violent reactions) may continue to burn for many seconds to minutes, depending on size and burning rate at ambient pressure.

PROPULSION

Propulsion of the munition or munition system may result from fairly stable internal burning at a pressure sufficient to cause choked flow at one or more openings, yet insufficient to burst the case. Propulsion may precede a case burst if the combustion pressure continues to rise fairly slowly or if openings are subsequently blocked by mechanical means.

DEFLAGRATION

A "deflagration" is an explosion of moderate violence, in which typically end closures are dislodged, the case appears to be torn rather than fragmented and some debris is thrown in excess of 15 meters. Burning pieces of EM will generally be thrown about. There may be some blast overpressure.

EXPLOSION

An explosion is usually characterized by a high internal pressure, case fragmentation into many moderate to small pieces – although fragments should show no evidence of plastic fracture. There will definitely be air shock waves. Debris may be thrown great distances. EM is usually consumed very rapidly – within a few milliseconds, although some may be thrown.

DETONATION

In a detonation, the case fragments will typically show evidence of plastic fracture due to very rapid failure at the pressure of the detonation wave, they will impact witness plates (within 1 meter) with sufficient velocities to cause cratering. All the energetic material will be consumed.

PARTIAL DETONATION

Evidence of partial detonation may result when an initial burning reaction grows to explosive pressures and thence transitions to a detonation prior to case burst.

10. COOKOFF MODELING CODES

Skocypec, et. al. presented what is arguably the best, brief summary of the many requirements for complete cookoff model development.[22] Most of the issues highlighted by Skocypec are treated in the analytical steps of this protocol. Complete cookoff models require coupling of the relatively slow heating phase to the ignition, slow-burn (conductive burn), accelerated-burn (convective/compressive burn), and (if necessary) DDT phase, and finally shock propagation of detonation through the thermally damaged EM. It is a point of discussion whether this should be accomplished in a single code-model, coupled codes for different rate domains, or separate codes run in sequence for each domain.

There is always the risk that in dealing with the complexities of sophisticated codes one might overlook important design details that the codes do not deal with. It is hoped that some of the design problems and approaches discussed earlier in this protocol will reduce that risk.

A survey of codes related to cookoff modeling by Dimaranan, et. al. in 1992 can be found elsewhere.[23]

REFERENCES

1. Diede, A. and Victor, A., "Propellant and Rocket Motor Behavior in Low Heating Rate Thermal Environments," presented to the Technical Cooperation Program (TTCP) Subgroup W Action Group (WAG-21) on The Hazards of Energetic Materials and Their Relation to Munitions Survivability, Adelaide, Australia, 13-17 March 1989.

2. Chapman, A.J., *Heat Transfer*, 4th Edition, Macmillan, 1984.

3.Pitts, D.R. and Sissom, L.E., *Heat Transfer*, Schaum's Outline Series, McGraw-Hill, 1977,

4. Chopey, N.P., *Handbook of Chemical Engineering Calculations*, 2nd Edition, McGraw-Hill, 1994.

5. *SFPE Handbook of Fire Protection Engineering*, National Fire Protection Association, 1992.

6. Drysdale, D., *An Introduction to Fire Dynamics*, John Wiley, 1985.

7. *Proceedings of the 1993 NIMIC Workshop on Cookoff*, NIMIC-S-395-93, Dimaranan, L.F., Heimdahl, O.E.R., and Covino, J., "An Assessment of Cookoff Modelling and Codes," pp. 305-316., 1993.

8. Victor Technology, *Guide to Spreadsheet Calculations for Insensitive Munitions Applications*, Victor Technology, Ridgecrest, California, July 1994.

9. Victor, A.C., "Exploring Cookoff Mysteries," 1994 JANNAF Propulsion Systems Hazards Subcommittee Meeting, San Diego, California, 1-4 August 1994.

10. Creighton, J.R., "The Variation of the Ignition Temperature of Solid Explosives as a Function of Heating Rate," 1993 JANNAF Propulsion Systems Hazards Subcommittee Meeting, CPIA Publ. 599, April 1993.

11. Koo, J.H., Miller, M.J., and Kneer, M.J., "The Effect of Hydrocarbon Flames to Fire Retardant Materials," Combustion Fundamentals and Applications, Joint Technical Meeting, Central and Eastern States Sections of the Combustion Institute, 15-17 March 1993. Also see "Behavior of Insulative Material Structures under simulated Fast Cookoff Environment," same authors, 1991 JANNAF Propulsion Systems Hazards Subcommittee Meeting, CPIA Publ. 562, March 1991.

12. Mangum, M.G., Cherry, C.C., and Wiechering, R.E., "Combustion Behavior of Reduced Smoke Propellant Under Cookoff Conditions," ADPA 1994 Insensitive Munitions Technology Sympossium, Williamsburg, Virginia, June 6-9, 1994, Proceedings, pp. 191-199.

13. Kernen, P. and NIMIC Staff, *Ways and Means to Insensitive Munitions - IM Recipes*, NIMIC-PK-425-93, October 31, 1993.

14. Brunet, J. "Modelling Associated with SNPE Tests," see Ref. 7, pp. 131-142.

15. Butcher, G.A., "Propellant Response to Cookoff as Influenced by Binder Type," AIAA 90-2524, AIAA/SAE/ASME/ASEE 26th Joint Propulsion Conference, Orlando, Florida, 16-18 July 1990. (also see "Propellant Response to Cookoff as Influenced by Binder Type, Part II Effects of Confinement" 1991 JANNAF Propulsion Systems Hazards Subcommittee Meeting, Albuquerque, New Mexico, 18-22 March 1991.)

16. Victor, A.C., "Chapter 9, Insensitive Munitions Technology for Tactical Rocket Motors," *Tactical Missile Propulsion*, AIAA Series Progress in Astronautics and Aeronautics, Washington, D.C., manuscript draft date: June 1994.

17. Farmer, J., et al, "A Study of Rocket Motors and Large-Scale Hazards Testing for the Insensitive Munitions Advanced Development (IMAD) Propulsion Program", NWC-TP 6840 (1988), Naval Weapons Center, China Lake, CA, USA.

18. Sandusky, H.W. and Bernecker, R.R., "Compressive Reaction in Porous Beds of Energetic Materials," Eighth Symposium (International) on Detonation, Naval Surface Warfare Center, NSWC MP 86-194, pp. 881-891, 1985.

19. Boggs, T.L. and Dickinson, C.W.,*The Hazards of Energetic Materials and Their Relation to Munitions Survivability*, The Technical Cooperation Program (TTCP), Summary Report on Workshop held at DREV, 5-9 OCtober 1992.

20. McAfee, J.M. and Asay, B.W., "Deflagration-to-Detonation in Granular HMX: Kinetics and Ignition in the Predetonation Region," Tenth International Detonation Symposium, Boston, Massachusets, 12-16 July, 1993.

21. Dhillon, M.S., Weyland, H.H., and Miller, R.R., "Insensitive Munitions Rocket Motor," ADPA 1994 Insensitive Munitions Technology Symposium, Williamsburg, Virginia, Proceedings, pp. 462-472, 6-9 June 1994.

22. Skocypec, R.D., et al, "An Evaluation of Cookoff, Status and Direction," 1991 JANNAF Propulsion Systems Hazards Subcommittee Meeting, Albuquerque, New Mexico, 18-22 March 1991, Chemical Propulsion Information Agency Publ. 562, March 1991.

23. Dimaranan, L.F., Heimdahl, O.E.R, and Covino, J., "An Assessment of Cookoff Modelling and Codes," JANNAF Workshop on Cook-off Mechanistic Understanding and Predictive Capabilities, CPIA Publ. 586, pp. 45-55, April 1992.

24. Kinney, G.F. and Graham, K.J., *Explosive Shocks in Air*, Springer-Verlag, New York, 1985.

25. Victor, A.C. *Warhead Performance Calculations*, Victor Technology, July 1993.

26. Baker, W.E., *Explosions in Air*, Wilfred Baker Engineering (Second Printing of 1973 edition, 1983).

27. Kuo, K.K. and Kooker, D.E., "Coupling Between Nonsteady Burning and Structural Mechanics of Solid-Propellant Grains," *Nonsteady Burning and Combustion Stability of Solid Propellants*, Edited by L. DeLuca, E.W. Price, and M. Summerfield, Progress in Astronautics and Aeronautics, Volume 143, American Institute of Aeronautics and Astronautics, Washington, D.C., 1992.